

# **Broadcast Signal Direction Finder**

Pei-Hung Tsai

A project report submitted to the Department of Electrical Engineering,  
University of Cape Town, in fulfilment of the requirements  
for the degree of Bachelor of Science in Engineering.

Cape Town, October 2008

# Declaration

I declare that this broadcast signal direction finder project report is my own, unaided work. It is being submitted for the degree of Bachelor of Science in Engineering in the University of Cape Town. It has not been submitted before for any degree or examination in any other university.

Signature of Author .....

Cape Town  
20 October 2008

# Abstract

Direction finding systems are used for locating, tracking and distinguishing various radio transmissions by means of radio direction finders. The purpose of this research is to study and compare the interferometer and triangulation techniques for direction finding, and building a receiver with a USRP board that can be utilised with GNU Radio software to receive signals from two antennas, separated in the horizontal plane. Modern techniques such as interferometer and triangulation using time difference of arrival are studied in detail, and compared with one another.

Simulations were done with interferometer and triangulation techniques by means of the FERS software. After the simulation was done, the results were compared and the interferometer has a better accuracy in terms of angle of arrival but it cannot locate the position of the target (transmitter). However, the triangulation technique has a poorer accuracy than the interferometer technique but it can locate the position of the target.

An interferometer is built with two FM antennas, two amplifiers, two bandpass filters, two basic RX boards and a USRP board. The receiver is utilised with GNU Radio software to receive signals from two antennas and compare the phase difference between two antennas.



In memory of my father

Ching-Ming Tsai

1953–1999



Many thanks to my mother

Shu-Chen Tsai

for her contribution towards my tertiary education

# Acknowledgements

I would like to express my gratitude to the following people for their assistance:

My supervisor, Professor Mike Inggs and Dr. Yoann Paichard.

All the people in the Radar and Remote Sensing group, who have helped in various ways, from discussing technical details to participating in experiments. In particular, Gunther Lange, Jonathan Ward, Sebastiaan Heunis and Lance for their sustained interest and input.

# Contents

<b>Declaration</b>	<b>i</b>
<b>Abstract</b>	<b>ii</b>
<b>Acknowledgements</b>	<b>v</b>
<b>List of Symbols</b>	<b>xi</b>
<b>Nomenclature</b>	<b>xii</b>
<b>1 Introduction</b>	<b>1</b>
1.1 Background to research . . . . .	1
1.2 Objectives . . . . .	2
1.3 Scope and limitations . . . . .	2
1.4 Plans of development . . . . .	2
<b>2 Direction finding</b>	<b>4</b>
2.1 Introduction . . . . .	4
2.2 Basic principles . . . . .	5
2.3 Direction finding techniques . . . . .	6
2.3.1 Interferometer technique . . . . .	6
2.3.2 Triangulation technique . . . . .	13
2.3.3 Relationship between interferometer and triangulation technique . . . . .	16
2.3.4 Other techniques . . . . .	18
2.3.5 Accuracy of an interferometer in noise . . . . .	18
2.4 Direction finding error source . . . . .	19
2.4.1 Propagation-induced errors . . . . .	20
2.4.2 Environmental errors . . . . .	20



---

2.4.3	Instrumental errors . . . . .	21
2.4.4	Observational errors . . . . .	21
2.5	Applications . . . . .	21
<b>3</b>	<b>Filter Design</b>	<b>23</b>
3.1	Objectives . . . . .	23
3.2	Design . . . . .	24
3.2.1	Prototype . . . . .	24
3.2.2	Filter Scaling and Transformation . . . . .	24
3.2.3	Bandpass filter design . . . . .	26
3.2.4	Construction . . . . .	29
<b>4</b>	<b>Simulations</b>	<b>35</b>
4.1	Pre-setup . . . . .	35
4.2	Simulation setup . . . . .	36
4.2.1	Interferometer . . . . .	36
4.2.2	Triangulation . . . . .	36
4.3	Results . . . . .	37
4.3.1	Interferometer . . . . .	37
4.3.2	Triangulation . . . . .	41
4.3.3	Comparison . . . . .	43
<b>5</b>	<b>Experimentation</b>	<b>46</b>
5.1	Pre-Setup of interferometer . . . . .	46
5.1.1	USRP . . . . .	46
5.1.2	GNU-Radio . . . . .	47
5.2	Interferometer design . . . . .	47
5.2.1	Antenna . . . . .	47
5.2.2	Amplifier . . . . .	48
5.2.3	Filter . . . . .	48
5.2.4	Receiver . . . . .	48
5.3	Testing . . . . .	48
5.4	Final Experiment . . . . .	56
5.4.1	Software . . . . .	56
5.4.2	Results . . . . .	58

---



<b>6</b>	<b>Conclusions</b>	<b>60</b>
<b>7</b>	<b>Future Work</b>	<b>61</b>
<b>A</b>	<b>Software Source Code</b>	<b>62</b>
	<b>Bibliography</b>	<b>69</b>

# List of Figures

2.1	direction finding co-ordinate convention [3] . . . . .	6
2.2	Interferometer direction finding technique - Delay [3] . . . . .	7
2.3	$\Delta\psi$ versus $\phi$ for different $d$ . [3] . . . . .	9
2.4	$\Delta\psi$ versus $\phi$ showing wrapping for $d=6m$ at 30MHz [3] . . . . .	10
2.5	Antenna response plot for 2 element array [3] . . . . .	12
2.6	Interferometer technique - time delay [4] . . . . .	13
2.7	Triangulation direction finding technique . . . . .	15
3.1	Maximally flat and equal-ripple low-pass filter responses ( $N=3$ ) [9]. . . . .	24
3.2	Bandpass filter circuit [9]. . . . .	26
3.3	Prototype beginning with a series element [9]. . . . .	27
3.4	Ansoft produced frequency response . . . . .	28
3.5	Inductance at 100MHz on the smith chart. . . . .	30
3.6	3dB bandwidth of the filter . . . . .	31
3.7	Filter response attenuation. . . . .	32
3.8	Resonance frequency of a straight wire . . . . .	33
3.9	Resonance frequency of a inductor (winded wire) . . . . .	34
4.1	Phase difference zoomed out . . . . .	38
4.2	Phase difference zoomed in . . . . .	39
4.3	Close up view of phase difference . . . . .	40
4.4	Signal one correlate with signal two . . . . .	41
4.5	Signal one correlate with signal three . . . . .	42
4.6	Signal one correlate with signal four . . . . .	42
4.7	Positions of the transmitter and the receivers . . . . .	44
4.8	Position of the transmitter and the receivers with the angle of arrival . . . . .	44



5.1	FM band	49
5.2	FM band with filter	49
5.3	Peak Power at 88.2MHz	50
5.4	Band Power at centred at 88.2MHz	50
5.5	FM band (with amplifier)	51
5.6	Peak power at 96MHz	51
5.7	Band Power at 88.2MHz with Amplifier	52
5.8	FM band	52
5.9	FM band with filter	53
5.10	Peak power at 88.2MHz	53
5.11	Band Power at 88.2MHz	54
5.12	FM band	54
5.13	Band Power at 88.2MHz	55
5.14	Power around 96MHz	55
5.15	Real and Imaginary from scope	57
5.16	Real and imaginary (different time divisions)	57
5.17	FFT of the signal received by the USRP (receiver)	58
A.1	Attenuation versus normalised frequency for 3.0dB ripple level [9]	63
A.2	Element values for 3.0dB Equal Ripple low-pass Filter Prototypes [9]	63
A.3	Prototype Filter Transformation [9]	64
A.4	Bandpass filter construction	65
A.5	Receiver construction	66
A.6	Receiver construction	67
A.7	2 Array Yagi Antenna	68

# List of Symbols

$\phi$	—	Angle of Arrival
$\Delta\psi$	—	Phase difference
$c$	—	Speed of light
$d$	—	Antenna separation distance
$\lambda$	—	Wavelength
$\Delta t$	—	Time delay
$R_0$	—	Source resistance
$\omega$	—	Angular frequency [rad/s]
$\delta$	—	Linear resolution
$\Delta$	—	Angular resolution
$\Gamma$	—	Signal to noise power ratio
$A$	—	Input signal magnitude
$\chi$	—	time bandwidth product
$\sigma_\varepsilon^2$	—	Asymptotic formula

# Nomenclature

**ADC**—Analog and digital converter.

**Azimuth**—Angle in a horizontal plane, relative to a fixed reference, usually north or the longitudinal reference axis of the aircraft or satellite.

**Beamwidth**—The angular width of a slice through the mainlobe of the radiation pattern of an antenna in the horizontal, vertical or other plane.

**DAC**—Digital to analog converter.

**DF**—Direction finding.

**DOA**—Direction of Arrival.

**Doppler frequency**—A shift in the radio frequency of the return from a target or other object as a result of the object's radial motion relative to the radar.

**DTOA**—Differential time of Arrival.

**FM**—Frequency Modulation

**RF**—Radio frequency.

**RX**—Receiver.

**SNR**—Signal to noise ratio.

**TDOA**—Time difference of arrival.

**USRP**—Universal Software Radio Peripheral.

**VHF**—Very high frequency.

# Chapter 1

## Introduction

### 1.1 Background to research

Since the beginning of the twentieth century, the area of small-aperture radio direction finding has grown and evolved. Today, direction finding plays an important role in the broader areas of passive radio-location and radio-navigation. Many techniques have been formulated, and many operational systems have been developed to satisfy a wide variety of technical and operational requirements. For example, direction finding systems are used in public services, military, commercial and civilian applications [5].

Direction finding refers to the techniques and systems used for locating, tracking and distinguishing various radio transmissions by means of a radio direction finder. The direction finder is used to determine the direction (angle) of arrival of an incident electromagnetic wave as received at the direction finding site. Direction finding systems provide several important functions in modern electromagnetic wave systems [5, 3].

The primary purpose of this research is to find characteristics of different direction finding techniques. The emphasis is on fundamental principles of operation and basic performance capabilities between the different techniques.

Direction finding systems have steadily evolved over a few decades. First generation system, using amplitude and amplitude-to-phase techniques for direction finding information, have been used effectively for numerous applications. However, major performance limitations exist when used on ionospherically propagated signals. Second generation systems have concentrated on phase difference and time difference of arrival techniques and have benefited from advances in receivers, processors, components, and devices [5].

Direction finding techniques may be required with frequencies above 300MHz (VHF) in the near future as size of the host platform decreases and the demand for covertness increases. Also, the structure of modern uncooperative emissions will be a major driver in establishing future small aperture direction finding architecture [5].

## 1.2 Objectives

The Objectives of this research is to

- Study and locate the position of the transmitter
- Study and locate the angle of arrival from the transmitter to the receivers
- Compare the different techniques to measure the Azimuth Angle (angle of arrival)
- Find the best technique depending on the criteria (type of signal, accuracy etc.). System configuration is needed.
- Experiment using USRP board with the interferometer techniques.

## 1.3 Scope and limitations

Theory on direction finding will be studied in detail, it includes interferometer and triangulation techniques. Both interferometer and triangulation techniques will be studied by means of a simulation (FERS simulator). The interferometer will then be implemented by hardware. Filter designs will be studied in conjunction with the implementation of the interferometer hardware.

Time is the major limitation for the research. The project time limit is around thirteen weeks. Quality of hardware provided for the research such as wires, inductors and capacitors also contribute towards the limitations of this project.

## 1.4 Plans of development

- **Chapter 1 - Introduction** - This chapter provides a brief outline on what the project is about. This includes the background of research, objectives of this research, motivation, scope and limitations to this research and plans of development.

- **Chapter 2 - Direction finding** - The project will start with the literature review. Reviewing on techniques and systems that are used to locate, track and distinguish the various radio transmissions by means of a radio direction finder. The basic principles of direction finding and the different techniques on direction finding is discussed in chapter 2. This research mainly focuses on two techniques such as interferometer and triangulation technique which is discussed in greater detail in the next chapter.
- **Chapter 3 - Filter Design** - This chapter discuss about the bandpass filter design which is needed for this project when doing the actual experiments on direction finding with an interferometer. The chapter starts with basic theories of filter designs by first laying out the objectives of the filter design. Design prototypes and impedance scaling and frequency transformation are discussed. After discussion of basic theories, the design of the filter will be carried out that meets the objectives. After the design has been made based on the theory, component values that are picked need to be tested before the final construction can begin.
- **Chapter 4 - Simulations** - Both interferometer and triangulation techniques are studied by means of simulations. The software used to simulate the signals is called FERS simulator. After simulating the signals from FERS, the signals are imported to MATLAB for further implementation. MATLAB is used to implement the interferometer and triangulation techniques to find the angle of arrival from the receiver(s) to the transmitter and the position of the transmitter.
- **Chapter 5 - Experiments** - The interferometer is implemented with hardware by using 2 FM antennas, 2 coaxial cables, 2 amplifiers, 2 filters, 2 basic RX boards and a USRP board. The Gnu-Radio software is used in conjunction with the USRP board to process the signals that are received. The process starts with setting up the two antennas at the correct position on the roof. Connecting both amplifiers and filters with coaxial cables and attach one end on the antenna and the other end of the basic RX board that is already connected to the USRP. After setting up the hardware's, Gnu-Radios build in function 'Gnu-Radio oscilloscope' is used to check if any signals are captured. A program that is written by a postgraduate student from UCT is used in this experiment to process the data that are captured.
- **Chapter 6 - Conclusion** - This section describes what has been found in this research.
- **Chapter 7 - Future work** - This section suggests some future work that could be done to improve the system.

# Chapter 2

## Direction finding

### 2.1 Introduction

Direction finding refers to the techniques and systems used for locating, tracking and distinguishing various radio transmissions by means of a radio direction finder. The direction finder is used to determine the direction (angle) of arrival of an incident electromagnetic wave as received at the direction finding site [3, 5].

A normal direction finding system consist of 4 parts, namely the antenna, receiver, processor and a display system. The antenna is the main element of the system. It plays an important role in direction finding. The antenna may be composed of a single rotating antenna or an array of antennas (interferometer). If the array of antennas are used as one receiver, the signal characteristics could be measured to find the angle of arrival. Since these characteristics are unique for every angle of arrival in an antenna, the bearing can be determined by processing and analysing the antenna outputs by determining the phase. This will be discussed in detail later [4].

The direction finding antenna plays an important role in the performance of the overall system so it should be well designed and manufactured. In this project, we are using the already available FM antennas that are provided by the remote and sensing group[4].

A receiver is connected to the output of the antenna that may contain a amplifier if the received signal is too weak, and a narrow band filter which is used to filter out the unnecessary signals and to prevent aliasing. A USRP board used to provide a standard signal processing feature common to all receivers. The characteristics of the receiver depend on the objectives of the project. This will be discussed in detail later.

For a multiple-channel, phase and time differential direction finding system, the receiver is relatively complex, providing both analog and digital processing and parameter measurements [4].

Earliest direction finding systems used an antenna with a directional response pattern which was physically rotated. The direction of arrival of a signal was determined by noting the direction of the antenna for which the received signal was strongest [3].

Modern direction finding systems are based on high-performance ADCs and DSPs. Most make use of arrays of omnidirectional antennas [3]. The angle of arrival information can be extracted by processing and analysing the complex output voltages, since these characteristics are unique for every received azimuth information [4].

This chapter discusses both general radio direction-finding principles and direction finding techniques used for radio direction finding.

## 2.2 Basic principles

A direction finding (x,y) spatial coordinate system with the direction finding system located at the (0,0) point. The angle of arrival associated with the direction of arrival are the azimuth angle  $\phi$ , measured from the x axis. An ideal direction finder would be capable of working over a wide band, 360° of azimuth, dealing with all forms of modulation and of giving accurate and reliable bearing in two dimensions, considering that the earth is flat. The figure below shows the directing (x,y) with direction finding system at the (0,0) point [4].

In general, it is assumed that the electromagnetic field propagating towards the direction finding system is a far-field planar wave with linear polarisation. The behaviour of electric and magnetic components of an electromagnetic planar wave emitted from a current carrying wire are shown in the figure2.1 below [4].

A full-capacity direction finding system should measure the angle of arrival in three dimensional space. However, in many applications (and this project), only  $\phi$  is required in the azimuth (xy) plane. A one coordinate direction finding system provides angle of arrival information in only one plane, usually the azimuth plane. The measured angle of arrival  $\phi$ , is also called the bearing angle or azimuth angle. Bearing is defined as “the horizontal direction of one point from another, expressed as the angle in horizontal plane between a reference line and the horizontal project of the line joining the two points” [4].

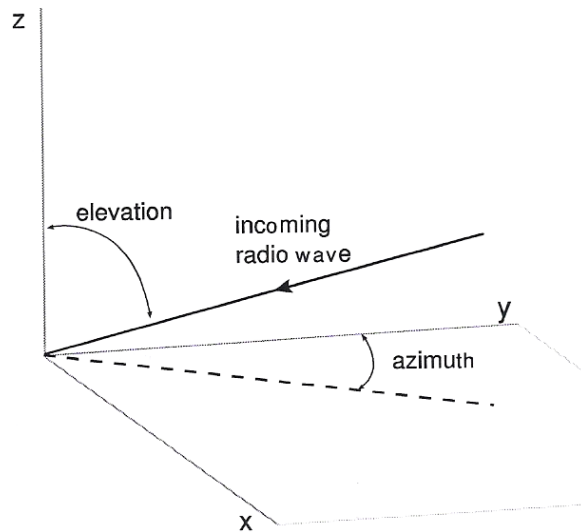


Figure 2.1: direction finding co-ordinate convention [3]

## 2.3 Direction finding techniques

Numerous techniques have been formulated and many operational systems have been developed to satisfy a wide variety of technical and operational requirements. Direction finding systems basically determine the angle of arrival information by three measurement methods such as amplitude response, phase delays and time delays. More complex techniques like the time difference of arrival technique and triangulation technique can also be used. Modern direction finding systems are composed of a direction finding antenna having an array of spatially distributed elements. When an emitter of interest is not at the bore-sight of the antenna, the output voltages produced by these elements will have some characteristics in terms of phase, amplitude or both [4].

### 2.3.1 Interferometer technique

Interferometer generally refers to an array type antenna (positioning few antennas equally or not equally spaced in a straight line. i.e. co-linear). Interferometer direction finding systems are utilised where accurate angle of arrival information is required. It has the advantage of having a fast response, but require relatively complex microwave circuitry, which must maintain a precise phase match over through a wide range of the frequency band. When high accuracy is required, wide baseline interferometers are utilised with ambiguity resolving circuitry [1].

#### Phase Method

Phase comparison direction finding systems determine the angle of arrival information by direct phase comparison of the signals received by separate antennas. At least two antennas are needed in

this case shown in the figure 2.2 below [4].

The antennas are  $d$  meters apart from each other and the incident wave is at an angle of  $\phi$ . The propagating wave is received at antenna 1 first and travels an additional distance to reach antenna 2. The distance can be determined by basic trigonometry, getting the result of  $d \sin \phi$ . The additional time that the signal needs to reach antenna 2 will create a phase difference between antenna 1 and antenna 2. If a plane wave arrives perpendicular to the array axis (i.e.  $\phi = 0^\circ$ ), then the phase difference will be zero since the signal will reach both antennas at the same time [4].

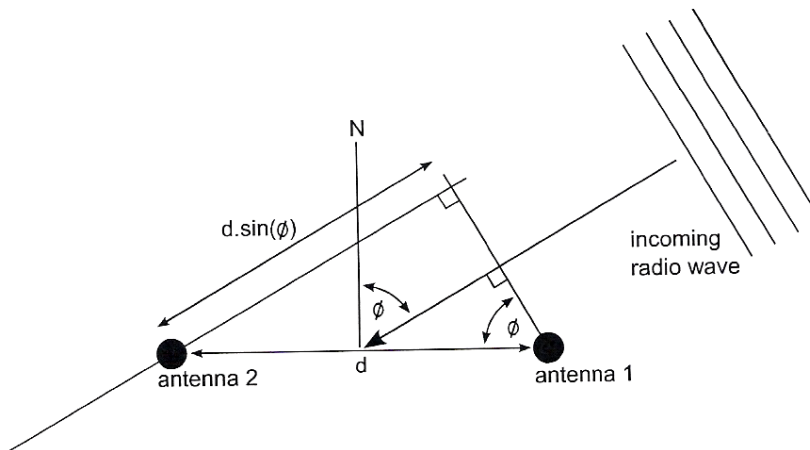


Figure 2.2: Interferometer direction finding technique - Delay [3]

The phase difference between the two signals can be expressed by

$$\Delta\psi = (2\pi d/\lambda) \sin\phi \quad (2.1)$$

$$\phi = \arcsin(\Delta\psi\lambda/2\pi d) \quad (2.2)$$

where  $\phi$  is the angle of arrival in radians,  $d$  is the antenna separations, and  $\lambda$  is the wavelength in metres [1].

The bearing angle  $\phi$  can be estimated by measuring the phase difference and replacing it in the formula given. It is assumed that the distance  $d$  between antennas and wavelength  $\lambda$  are known [4]. A phase comparator is used to measure the phase difference,  $\Delta\psi$ , between antenna channels. The outputs of each antenna elements are received and processed to convert to an IF signal before entering to the inputs of the phase comparator [4].

The unambiguous field of view is given by  $\phi = 2\sin^{-1}(\frac{\pi}{2d})$  which for  $\frac{\lambda}{2}$  spacing results in  $180^\circ$  coverage. This spacing must be established for the highest frequency to be received [1].

Interferometer elements typically use broad antenna beams with beam-width of around  $90^\circ$ . This lack of directivity produces adverse effects such as limiting the systems sensitivity due to the low antenna gain and it opens the system to interference signal from within the antenna's broad angular coverage. The interference signals often include multipath from strong signals which can limit the accuracy of the interferometer [1].

For two-element interferometer, the spacing  $d$  must be  $\frac{\lambda}{2}$  or less to provide unambiguous, or single lobe  $\pm 90^\circ$  coverage. This sets a wide interferometer lobe which must be split by a large factor to achieve high accuracy. This imposes a requirement for high SNR to achieve the large beam-splitting factor [1].

When high accuracy is required from an interferometer system, it is usual to employ separations greater than  $\frac{\lambda}{2}$ . The increased separation sets up a multi-grating-lobe structure through the coverage angle which requires less SNR to achieve a specified accuracy [1].

Interferometers employing multiple antenna elements are called multiple-baseline interferometers. In a typical design, the receiver consists of a reference antenna and a series of companion antennas. The spacing between the reference element and the first companion antenna is  $\frac{\lambda}{2}$ ; other secondary elements are placed to form pairs separated by 1, 2, 4 and 8 wavelengths [1].

The initial angle of arrival is measured unambiguously by the shortest spaced antenna pair that must be less than  $\frac{\lambda}{2}$ . The greatest spaced pair has a phase rate of change which is twice that of the first, but the information is ambiguous due to there being twice as many lobes as in the preceding pair. A greater phase rate of change permits higher angular accuracy while the ambiguity is resolved by the previous pair. Thus, the described multiple-baseline interferometer provides a binary angle of arrival measurement where each bit of the measurement supplies a more accurate estimate of the emitter's angle of arrival [1].

Interferometer direction finding accuracy is determined by the widest baseline pair. Typical cavity-backed spirals, track to 6 electrical degrees, and associated receivers track to  $9^\circ$ , resulting in an rms total of  $11^\circ$ . At a typical SNR of 16dB, the rms phase noise is approximately 9 electrical degrees. For these errors and an emitter angle of  $45^\circ$ , a spacing of  $25\lambda$  is required for  $0.1^\circ$  rms accuracy while a spacing of  $2.5\lambda$  is needed for  $1^\circ$  accuracy [1].

Figure 2.3 shows the  $\Delta\psi$  versus angle of arrival  $\phi$ , with  $\lambda = 10m$ , for 3 different baselines 1m, 4.5m and 6m respectively. This corresponds to  $0.1\lambda$ ,  $0.45\lambda$  and  $0.6\lambda$  for  $f = 30MHz$  [3].

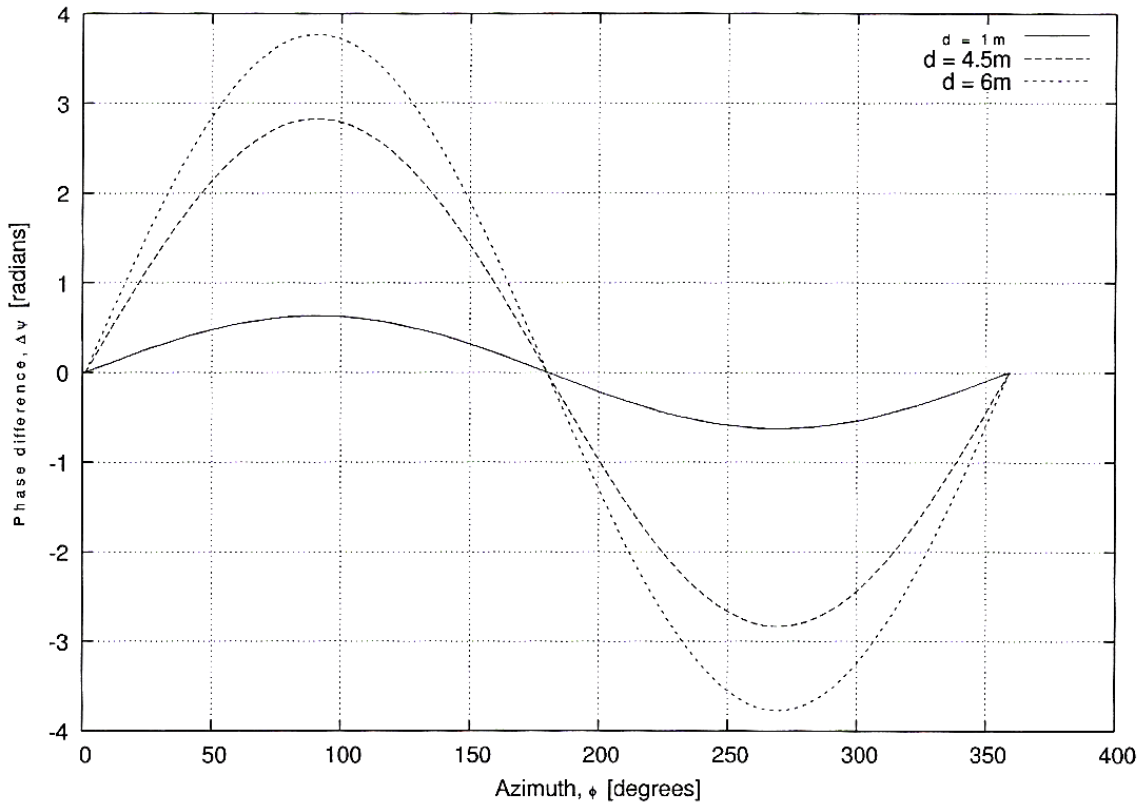


Figure 2.3:  $\Delta\psi$  versus  $\phi$  for different  $d$ . [3]

The first thing to notice is that with only 2 antennas, there is a  $180^\circ$  direction of arrival ambiguity; We cannot tell the difference between a signal with a direction of arrival of  $\theta^\circ$  and  $(180 - \phi)^\circ$ . This is easily resolved by using an additional antenna. An additional antenna also helps improve accuracy over ranges where the rate of change of  $\Delta\psi$  is small. The second thing to notice is that the maximum phase difference increases with increasing  $d$ . This impacts on precision. A system with  $d = 0.45\lambda$  is preferred to  $d = 0.1\lambda$ , since for a given direction of arrival error, the phase-difference resolution requirements are more relaxed. In other words, given a fixed phase difference resolution, the first system will have a smaller error on the direction of arrival measurements [3].

The phase difference measurements are restricted to a  $2\pi$  range. The plot of the  $0.6\lambda$  graph is out of range. The real plot of the  $0.6\lambda$  measurement is shown in figure 2.4.

So for  $d > 0.5\lambda$  an additional ambiguity is introduced. So a phase difference of  $3\pi$  corresponds to

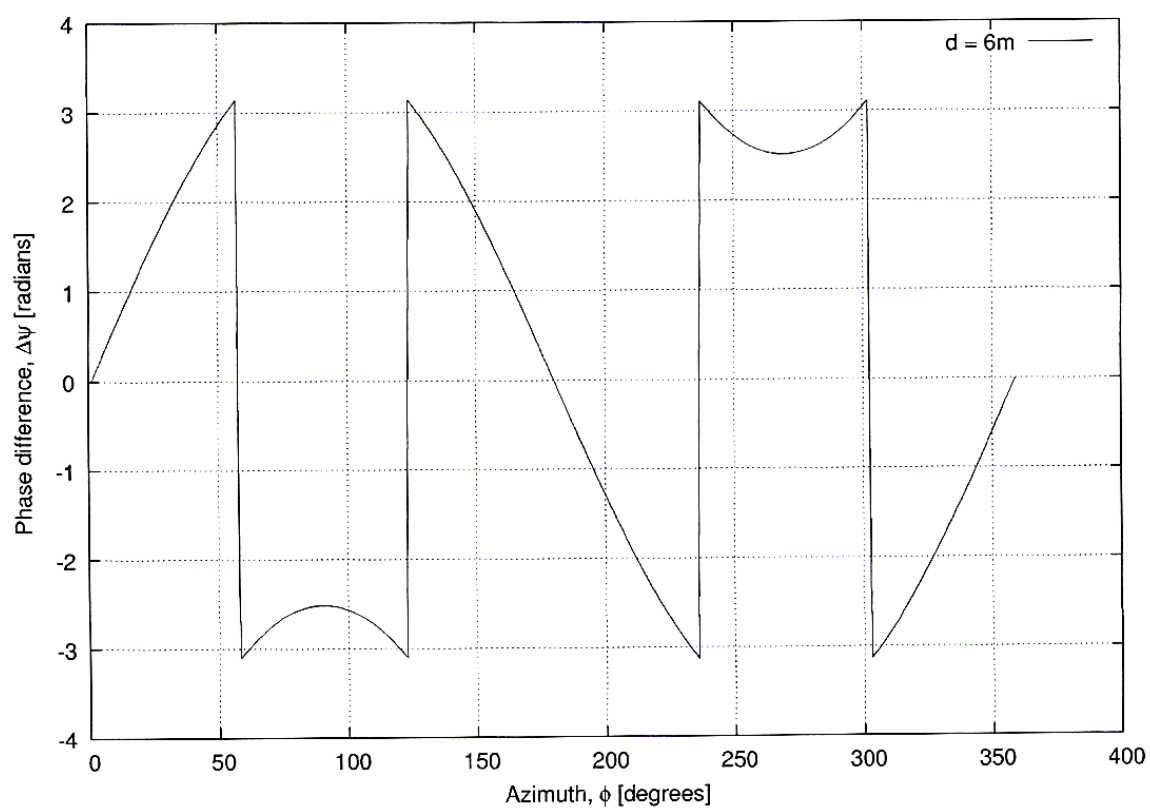


Figure 2.4:  $\Delta\psi$  versus  $\phi$  showing wrapping for  $d=6m$  at 30MHz [3]

azimuths of approximately  $53^\circ$ ,  $127^\circ$ ,  $241^\circ$  and  $299^\circ$ . Two of these are due to the previous ambiguity mentioned above [3].

Another way of looking at this is if we plot the magnitude of the sum of signals on the two antennas, it is shown in figure 2.5.

Consider what happens when  $d$  is increased. Initially, when the baseline is 1m, the response almost has the same shape as a single antenna except that the gain has doubled. When  $d = 1$ , the response has no directivity. When baseline is increased to 4.5m, the response changes. The response is strong for directions perpendicular to the baseline, and weak for directions parallel to the baseline. So the  $180^\circ$  direction of arrival ambiguity is evident [3].

As  $d$  increases and past  $\frac{\lambda}{2}$ , two additional side lobes appear which increases in size as  $d$  increases. These side lobes correspond to the ambiguity mentioned earlier. Also notice that the original lobes are narrower - this corresponds to increased angular resolution. If  $d > \lambda$ , more side lobes will appear which introduces further ambiguity [3].

To summarise, a direction finding system that uses phase-difference method will need at least 3 antennas. At least one pair of antennas should have a baseline less than  $0.5\lambda$ , and in practise this is typically further reduce to  $0.4\lambda$  to compensate for measurement noise. Adding an additional antenna pair with larger baselines improves angular resolution [3].

### Time delay measurements

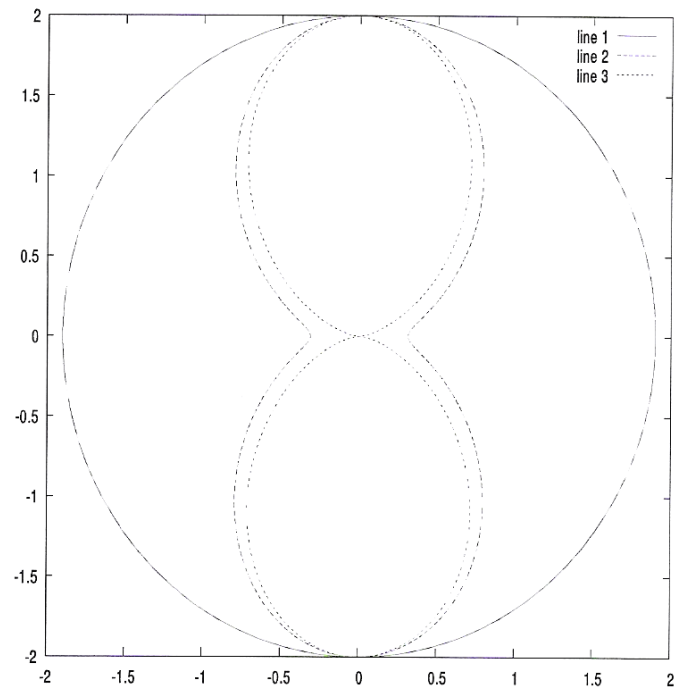
Time delay and phase delay are related to each other, they both use the interferometer technique to find the angle of arrival and time delay can be estimated from a phase measurement if the wavelength and the velocity (normally the speed of light,  $3 \times 10^8$ ) of the propagating wave is known. Instead of measuring the phase difference as in the previous method, it measures the time difference of arrival at two antennas. Figure 2.6 shows a direction finding system with two antennas where the time delay,  $\Delta t$  between the two antennas in [4] is given by

$$\Delta t = \left(\frac{d}{c}\right)\sin\phi$$

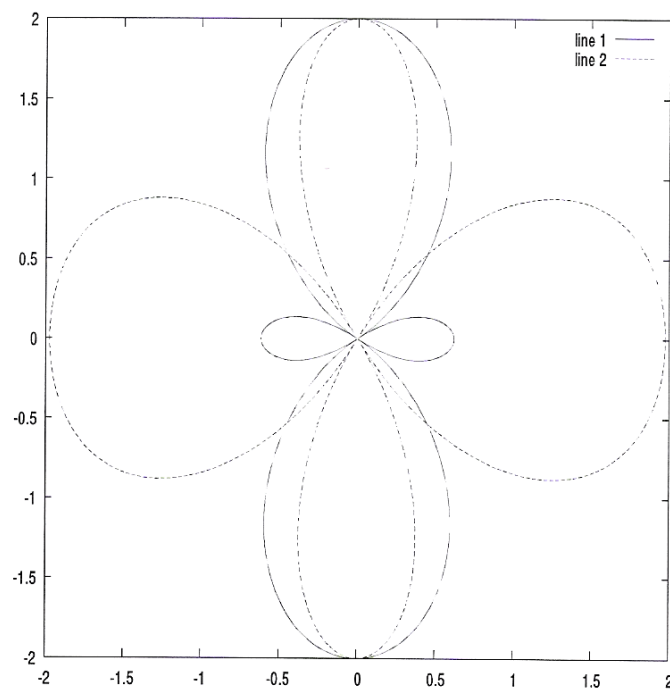
so rearranging it,

$$\phi = \arcsin\left(\frac{c\Delta t}{d}\right)$$

Where  $\phi$  is the bearing angle,  $d$  is the distance between two antennas and  $c$  is the speed of light [4].



a) baselines: line 1 = 1m, line 2 = 4.5m, line 3 = 5m



b) baselines: line1 = 6m, line2 = 9.5m

Figure 2.5: Antenna response plot for 2 element array [3]

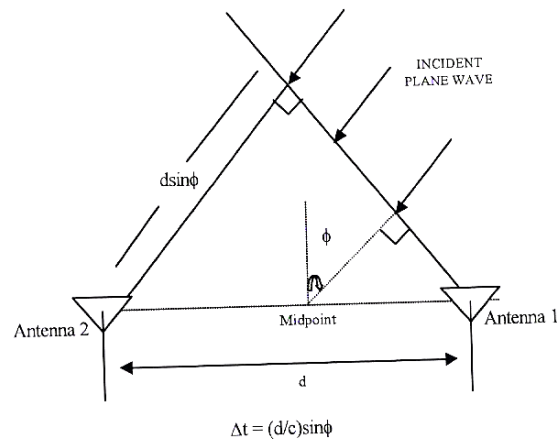


Figure 2.6: Interferometer technique - time delay [4]

### 2.3.2 Triangulation technique

The emitter (transmitter) identification function requires identifying and associating consecutive pulses produced by the same emitter in angle of arrival and frequency. The angle of arrival is a parameter which a hostile emitter (transmitter) cannot change on a pulse-to-pulse basis. However, to measure the angle of arrival of pulses which overlap in the time domain first requires them to be separated in the frequency domain [7].

This is a location technique involving only angle measurements taken from more than one observation site. Triangulation is used in moving observation systems consisting of single measuring platform or stationary systems consisting of two or more measuring platforms [7].

This is where the intersection of successive spatially displaced bearing measurements provides the emitter location. Time difference of arrival which measures the difference in time of arrival of a single pulse at three or more spatially remote locations [1].

This technique is very flexible in use. It may be utilised to locate emitters operating either with continuous wave signal or pulse signals. Triangulation minimises the effect of random data measurement errors on estimate of emitter position but is vulnerable to DF systematic errors (bias). Triangulation is used effectively to locate ground emitters by moving or stationary measuring platforms in the presence of pure random measurement errors. The methods are very sensitive to systematic measurement errors [7].

The range difference (hyperbolic) ELM is based on time difference of arrival (TDOA) measurements only. TDOA approach requires three or more measuring platforms that cooperate in emitter position determination. TDOA technique utilises measurements of the time of arrival pulsed signals at three

or more spatially separated receivers. Time difference of arrival measurement value is determined on the plane of an isodelay curve (hyperbolic). The hyperbolic location technique based upon TDOA measurements can be used to locate emitters of pulsed signals only [7].

Time difference of arrival measurement error influences on the emitter location error. For pulsed signals, the error in TDOA measuring strongly depends on the bandwidth of the measurement channel. If the bandwidth is wider then the error will be smaller. Therefore very short pulses are preferred for very accurate TDOA measurements [7].

The main advantage of the range-difference (hyperbolic) ELM based upon TDOA measurements, realised in the system with long baselines, is that the most accurate and paid emitter location may be provided because of relatively easy and accurate measurements of time delay. This technique requires at least three simultaneously operating platforms, high quality receivers, wide-band data link between the platforms, very high performance central processor and very high reliability of cooperating subsystems. It is very useful to locate emitters generating pulsed signals, but it can not be used to locate CW-type emitters [7].

The most widely used position location technique for geolocation of mobile users is the hyperbolic position location technique, also known as the time difference of arrival position location technique. This technique uses a cross-correlation process to calculate the difference in time of arrival of a signal at multiple pairs of stations [2].

This delay defines a hyperbola of constant range difference from receivers, which are located at the foci. Each time difference of arrival measurement yields a hyperbolic curve along which the receiver may be positioned. When many receivers are used, multiple hyperbolas and the intersection of the set of hyperbolas will be formed. The following algorithm were derived in [2] but some adjustments have been made.

Lets assume that the transmitter is at an unknown position  $(x,y)$  reference to the University of Cape Town at  $(0,0)$  as shown in figure 2.7. The distance from the transmitter to UCT will be  $\sqrt{(x-x_0)^2 + (y-y_0)^2} = \sqrt{x^2 + y^2}$ , from [2], we can find

the distance

$$R_{A0} = \sqrt{(x-x_A)^2 + (y-y_A)^2} - \sqrt{x^2 + y^2}$$

$$R_{B0} = \sqrt{(x-x_B)^2 + (y-y_B)^2} - \sqrt{x^2 + y^2}$$

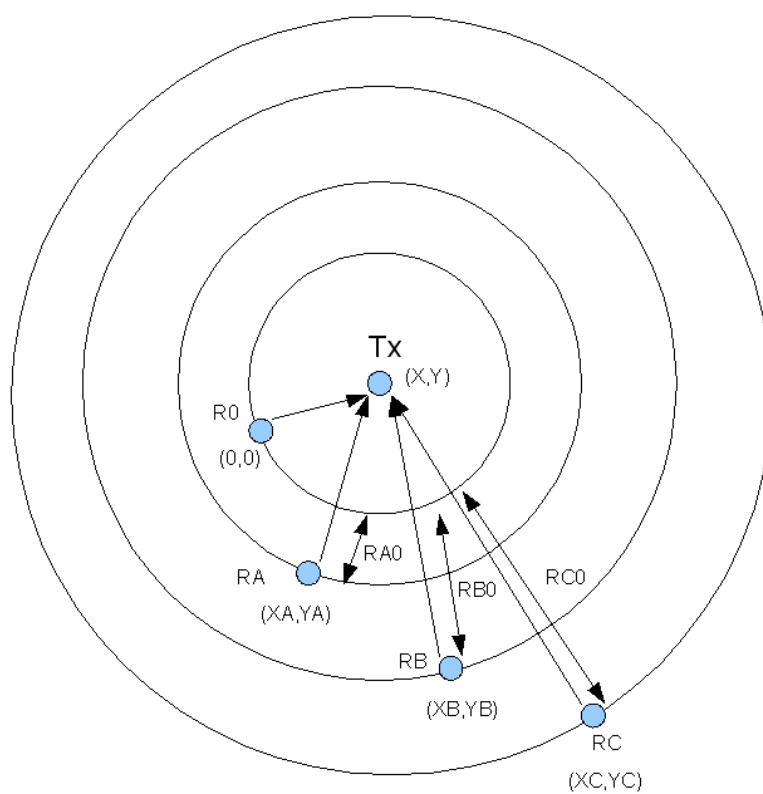


Figure 2.7: Triangulation direction finding technique

$$R_{C0} = \sqrt{(x - x_C)^2 + (y - y_C)^2} - \sqrt{x^2 + y^2}$$

Rearranging,

$$\sqrt{x^2 + y^2} = \frac{x_A^2 - 2x_Ax + y_A^2 - 2y_Ay - R_{A0}^2}{2R_{A0}}$$

$$\sqrt{x^2 + y^2} = \frac{x_B^2 - 2x_Bx + y_B^2 - 2y_By - R_{B0}^2}{2R_{B0}}$$

$$\sqrt{x^2 + y^2} = \frac{x_C^2 - 2x_Cx + y_C^2 - 2y_Cy - R_{C0}^2}{2R_{C0}}$$

Solving simultaneously,

$$y = x \left[ \frac{R_{A0}x_B - R_{B0}x_A}{R_{B0}y_A - R_{A0}y_B} \right] + \frac{R_{B0}[x_A^2 + y_A^2 - R_{A0}^2] - R_{A0}[x_B^2 + y_B^2 - R_{B0}^2]}{2[R_{B0}y_A - R_{A0}y_B]} \quad (2.3)$$

$$y = x \left[ \frac{R_{A0}x_C - R_{C0}x_A}{R_{C0}y_A - R_{A0}y_C} \right] + \frac{R_{C0}[x_A^2 + y_A^2 - R_{A0}^2] - R_{A0}[x_C^2 + y_C^2 - R_{C0}^2]}{2[R_{C0}y_A - R_{A0}y_C]} \quad (2.4)$$

These straight line equation shows the two point of intersection of the hyperbola. Make the two straight line equations equal will locate the position of the transmitter.

### 2.3.3 Relationship between interferometer and triangulation technique

The significantly cheaper alternative to phase interferometry offers some angle of arrival determination techniques using time difference of arrival measurements. The measurements are realised using a short baseline instead of the long baseline. Main advantages of TDOA direction-finding technique over phase interferometry is that angle of arrival calculation is independent of signal frequency. Moreover, phase ambiguities don't occur here, there is no need to use auxiliary resolving channels. In addition, because of very short time interval measurements, effect of multipath reflections is eliminated. This technique is sometimes called differential time of arrival. It requires extremely accurate time delay measurements [7].

In practise, the most often used emitter location techniques are angular (triangulation, azimuth/elevation) and range difference. For both angular emitter location technique, the better techniques seems to be

phase comparison (interferometer technique) and Differential time of arrival (DTOA). DTOA is the angle of arrival determination technique time-difference-of-arrival measurements realised using short baseline [7].

The most sophisticated emitter location techniques are based upon angle of arrival determination principle by phase comparison using theory of multiple baseline interferometry and very expensive interferometer structures. The interferometers are built as complex receiving systems providing digital signal processing at microwave frequencies. Advanced interferometer technology provides already very high accuracy of angle of arrival determination. Main problems are still related to elimination of angle of arrival determination ambiguity and to the necessity of accurate measurements of signal frequency before angle of arrival determination. This technique is preferable to precise location of emitters and it is currently applied in sophisticated land-based, airborne and shipborne ELINT system [7].

### **Interferometer [5]**

#### *Strengths*

- Nearly instantaneous bearing acquisition
- Relatively simple
- No antenna switching required

#### *Limitations*

- Susceptible to interference in the pass-band
- limited Field of view

### **Triangulation (TDOA) [5]**

#### *Strengths*

- Conceptually simple
- Independent of frequency
- Rapid direction of arrival acquisition
- Low power requirements

- Low operator proficiency needed

#### *Limitations*

- Modulation dependent
- Channel matching and tracking required
- Requires state-of-the-art time-interval measurements
- Broadband devices and components needed
- Performance degrades rapidly as SNR decreases
- Periodic calibration is necessary to maintain accuracy

### **2.3.4 Other techniques**

#### **Amplitude based**

This include systems with mechanically rotated antennas [3]. Amplitude response direction finding is realised by using two or more antennas. The antennas are configured in such a way that the relative amplitudes of the outputs are unique for all angle of arrival measurements. The important application of amplitude comparison direction finding technique is known as Watson Watt [4].

#### **Doppler based**

Doppler based direction finding systems make use of the fact that the received frequency at a moving antenna experiences a Doppler shift. This shift is a maximum for motion directly toward or away from the transmitter (emitter), and is zero for motion tangential to the transmitter. For stationary direction finding platforms the antenna can be physically rotated, or else a pseudo-Doppler technique is used, where the antenna input to the direction finding system is switched rapidly between a number of fixed antennas [3].

### **2.3.5 Accuracy of an interferometer in noise**

Interferometers base their estimates on measurements of the phase differences between signals from different sensors. The basic problem is to estimate the errors in these phase-difference measurements. The phase errors arise as a direct consequence of noise present in the signals received by the sensors and noise introduced by the signal amplifier. The phase errors are thus a function of the signal-to-noise power ratio prevailing at the amplifier outputs and the extent to which signal averaging is employed to improve it. Specifically, interferometer performance primarily depends on

two dimensionless quantities, namely the SNR and the time-bandwidth product in which time is the duration of the observations on the signals prior to making an estimate of the phase difference, and 'bandwidth' is the bandwidth occupied by the observed signals and noise [10].

By geometry, the phase error is

$$\varepsilon(t) = \arctan\{\rho_0(t)\sin\psi_0(t)/[A^2 + \rho_0(t)\cos\psi_0(t)]\}$$

where  $\rho_0(t)$  is the magnitude and  $\psi_0(t)$  is the instantaneous phase, of  $x(t)$  relative to the signal vector.

From [12], the signal-to-noise power ratio

$$\Gamma = \frac{A^2}{2}$$

and the time-bandwidth product is

$$\chi = 2BT$$

For a large  $A$  and large  $\chi$  the phase error variance approaches the well-known asymptotic formula.

$$\sigma_\varepsilon^2 \rightarrow \frac{2}{A^2\chi} = \frac{1}{\Gamma\chi}$$

so

$$\sigma_\varepsilon^2 = \frac{1}{SNR \times TB} \quad (2.5)$$

That is, the variance decreases reciprocally with both increasing SNR and with increasing TBP [10].

## 2.4 Direction finding error source

Direction finding systems are susceptible to a wide variety of direction of arrival error sources such as [5]

- Propagation-induced errors;
- Environmental errors;
- Instrumental errors;
- Observational errors.

As a signal travels from an radio frequency source to a direction finding system, direction of arrival errors accrue in the sequence listed above. The errors are cumulative because they originate from independent causes that involve statistical definitions. The error statistics for each error category are statistically combined to arrive at an overall error definition [5].

After transmission, a signal traverses the propagation medium, such as the ionosphere, which introduces direction-of-arrival deviations, time dispersion effects, and signal amplitude degradation. As the signal approaches the direction finding site, environmental errors occur when the signal encounters natural and man-made scattering and re-radiation objects that deviate the signal from a linear propagation path. At the direction finding system, the signal may experience instrumental errors caused by equipment imperfections such as antenna unbalance and antenna pattern distortions etc. [5]

## 2.4.1 Propagation-induced errors

### Propagation Mechanisms

Propagation induced errors are those created by the intervening media as the signal of interest propagates between the radio frequency source and the direction finding site. Electromagnetic waves propagate from a RF source to a direction finding site in four major ways such as ground, ionospheric, tropospheric and scatter propagation [5].

### Direction-of-arrival Errors

Very high frequency (VHF) direction finding use extends from about 30 to 300MHz. Medium aperture antennas must be used for frequency above 150MHz. At VHF, the surface wave is useless for direction finding purposes, and direction finding must be performed on direct, reflected or lateral waves. Operational VHF direction finding experience indicates that the direction of arrival of the direct wave is generally accurate and lies on, or close to, the great-circle bearing. Reflection BHF propagation can deviate widely from the linear propagation path and produce erroneous direction-of-arrival conditions. Error increases as surface roughness increases [5].

## 2.4.2 Environmental errors

Direction finding systems are often operated under conditions that are decidedly non-optimal. The direction finding site usually contains re-radiators, reflectors, surface obstructions etc. Environmental errors are introduced into the direction finding system in an integral part of its immediate environs and reacts to factors in the environs [5].

The errors produced by the far-region (more than  $10\lambda$ ) effects are uncontrollable in the sense that calibration corrections are not feasible and computational efforts are not profitable. If direction finding site is fixed, a long-term history of direction-of-arrival data on remote transmissions from known locations may provide some quantitative data on far-region error effects and may afford correction parameters [5].

### 2.4.3 Instrumental errors

Instrumental errors are created in the direction finding system as a result of either equipment imperfections or fundamental error mechanisms in the direction finding technique used. Equipment imperfections encompass a wide variety of factors including the following [5]:

- Low SNR;
- Amplitude and phase unbalance;
- Time and frequency inaccuracies;
- Hardware imperfections and ageing;
- Physical misalignment;
- Digital processing algorithm imprecision;
- Calibration inaccuracy

### 2.4.4 Observational errors

Observational errors are those that occur at the operator interface, and are not necessarily operator errors. Observational errors are due primarily to the inability of the direction finding read-out or display to present uncorrupted information to the operator. Observational errors apply primarily to analog read-outs and displays. Digital read-outs are assumed to have negligible observational error unless we want to consider visual acuity as an error source [5].

## 2.5 Applications

Direction finding as described in [3] is mainly used for:

- Civil: Radio-monitoring, searching for interference sources, localisation of non-authorised transmitters, air and marine navigation and wild life tracking

- Military: communication intelligence, force strength assessments, gaining information on an opponent's order of battle (signal intelligence) and friendly force location
- Security and Safety services: fight organised crime, search and rescue operations (emergency beacon location) and personnel vehicle location

Direction finding has become increasingly popular in commercial, civilian, governmental and military applications. It is important in the Communication Intelligence (COMINT) applications for military purposes. A successful electronic attack is possible if a successful electronic warfare support system is used to measure the direction to the victim emitter. Interference source location, emission control, frequency management, spectrum management are some other important application areas [4].

# Chapter 3

## Filter Design

Filters are two-port networks that are used to control the frequency response of an RF or microwave system by allowing transmission at frequencies within the pass-band of the filter, and attenuation within the stop-band of the filter. Common filter responses include low-pass, high-pass, bandpass and band stop. The filter that is needed in this project is a bandpass filter. This filter is used in the receivers for rejecting signals outside the operating band, attenuating undesired mixer products [9].

Many techniques have been proposed for the design and analysis of filter circuits, but in this project, insertion loss method is used because of the flexibility and accuracy that it provides. The insertion loss method is based on network synthesis techniques, and can be used to design filters having a specific type of frequency response. The technique begins with the design of a low-pass filter prototype that is normalised in terms of impedance and cutoff frequency. Impedance and frequency scaling and transformations are then used to convert the normalised design to the one having the desired frequency response, cutoff frequency, and impedance level (namely the bandpass filter that is required for this project) [9].

### 3.1 Objectives

The bandpass filter's centre frequency must sit at around 88.2 MHz (Typerberg's 5FM signal). The 3dB bandwidth must be 2 MHz and it must attenuate to around 30dB at a band of 16 MHz to prevent aliasing. The diagram below shows the graphical representation requirements of the filter design.

## 3.2 Design

### 3.2.1 Prototype

There are 3 types of low pass filter prototypes namely Maximally Flat, Equal-Ripple and Linear Phase low-pass filter prototype. The most commonly used are the Maximally Flat and Equal-Ripple filters. These two prototype performances has a trade-off. Maximally Flat provides the flattest possible pass-band but a lower attenuation while the Equal ripple has a sharper cut-off characteristic and higher attenuation but the pass-band response will have ripples of amplitude  $1+k^2$ . Figure shows the comparison between the Maximally flat and equal-ripple low-pass filter response [9].

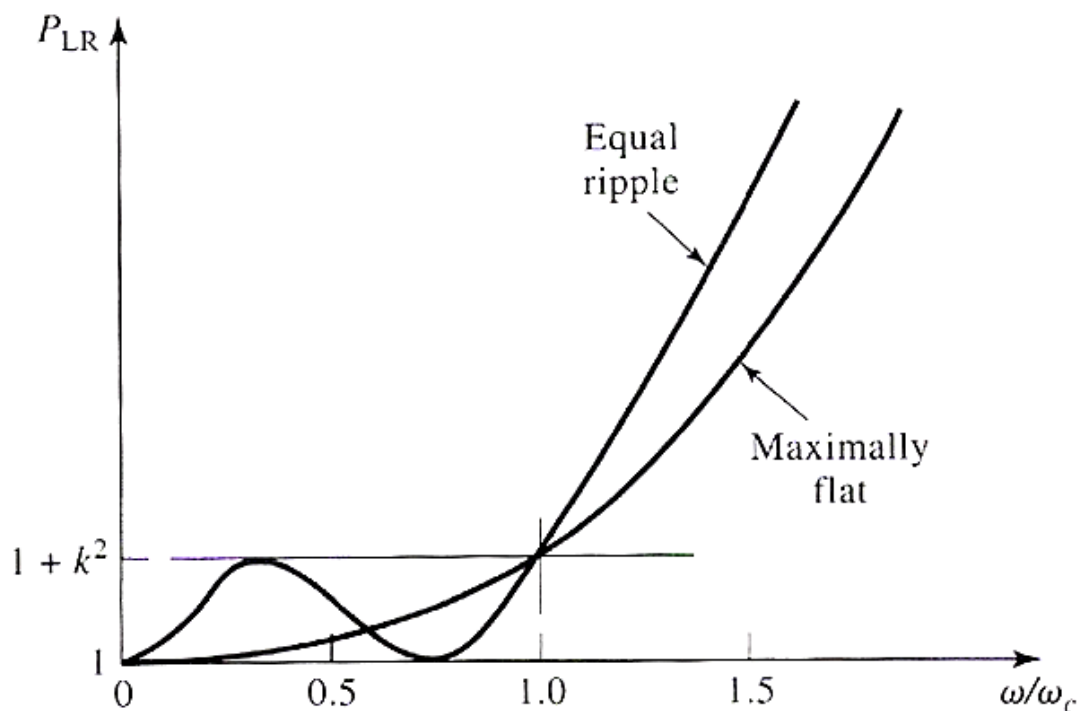


Figure 3.1: Maximally flat and equal-ripple low-pass filter responses (N=3) [9].

### 3.2.2 Filter Scaling and Transformation

In this section, the process of converting a normalised low-pass filter prototype to a filter circuit having a prescribed impedance level, cutoff frequency, and frequency response is described.

## Impedance Scaling

In the prototype design, the source and load resistances are unity (except for the case of equal-ripple filters with  $N$  even, which have non-unity load resistance). A source resistance of  $R_0$  can be obtained by multiplying the impedance's of the prototype design by  $R_0$ . [8]  $R_0$  in this case is set to  $75\Omega$  because the cables that are used to connect the antennas with the filters are  $75\Omega$  cables. Then, if we let primes denote impedance scaled quantities, we have the new filter component values given by

$$L' = R_0 L \quad (3.1)$$

$$C' = \frac{C}{R_0} \quad (3.2)$$

$$R'_s = R_0 \quad (3.3)$$

$$R'_L = R_0 R_L \quad (3.4)$$

where  $L$ ,  $C$ , and  $R_L$  are the component values for the original prototype [9].

## Bandpass Frequency Transformation [9]

Low-pass prototype filter designs can be transformed to produce the bandpass response. If  $\omega_1$  and  $\omega_2$  denote the edges of the pass-band, then a bandpass response can be obtained by using the following frequency substitution:

$$\omega \leftarrow \frac{\omega_0}{\omega_2 - \omega_1} \left( \frac{\omega}{\omega_0} - \frac{\omega_0}{\omega} \right) = \frac{1}{\Delta} \left( \frac{\omega}{\omega_0} - \frac{\omega_0}{\omega} \right) \quad (3.5)$$

from the above equation, the following equation can be derived

$$\omega \leftarrow \frac{\omega^2 - \omega_0^2}{(\omega_2 - \omega_1)\omega}, \quad (3.6)$$

where

$$\Delta = \frac{\omega_2 - \omega_1}{\omega_0}, \quad (3.7)$$

is the fractional bandwidth of the pass-band. The centre frequency  $\omega_0$ , could be chosen as the arithmetic mean of  $\omega_1$  and  $\omega_2$ , but the equations are simpler if it is chosen as their geometric mean, so

$$\omega_0 = \sqrt{\omega_1 \omega_2}. \quad (3.8)$$

Series inductor,  $L_k$ , in the low-pass prototype is transformed to a series LC circuit with element values given by

$$L'_k = \frac{L_k}{\Delta\omega_0}, \quad (3.9)$$

$$C'_k = \frac{\Delta}{\omega_0 L_k}. \quad (3.10)$$

Shunt Capacitor,  $C_k$ , in the low-pass prototype is transformed to a shunt LC circuit with element values given by

$$L'_k = \frac{\Delta}{\omega_0 C_k}, \quad (3.11)$$

$$C'_k = \frac{C_k}{\Delta\omega_0}. \quad (3.12)$$

The low-pass filter elements are thus converted to series resonant circuits in the series arms, and to parallel resonant circuits in the shunt arms. Both series and parallel resonator elements have a resonant frequency of  $\omega_0$ . Figure shows the circuit diagram after transformation from low-pass to bandpass [9].

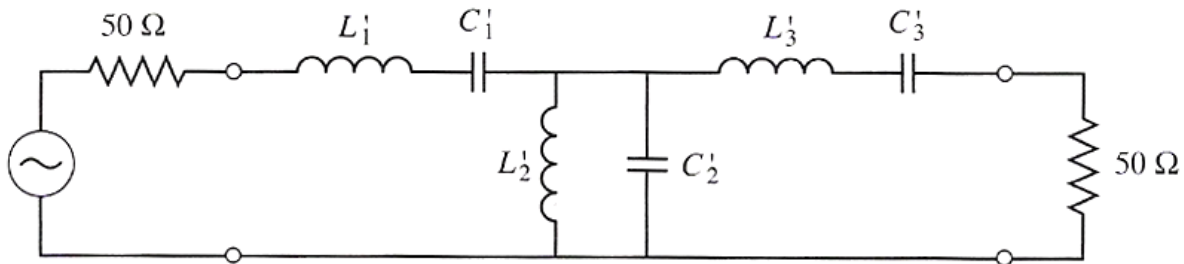


Figure 3.2: Bandpass filter circuit [9].

### 3.2.3 Bandpass filter design

From theory, we can obtain the frequency transformation  $\omega = \frac{\omega^2 - \omega_0^2}{(\omega_2 - \omega_1)\omega} = \frac{4\pi^2(f^2 - f_0^2)}{4\pi^2(f(f_2 - f_1))} = \frac{(f^2 - f_0^2)}{(f(f_2 - f_1))}$  where  $f = 100.5\text{MHz}$ ,  $f_0 = \sqrt{(82.5\text{MHz})(93.5\text{MHz})}$ ,  $f_2 = 93.5\text{MHz}$ ,  $f_1 = 82.5\text{MHz}$  and  $f_c = 1\text{MHz}$ . Substituting into the equation we get  $f = 2.16$ , and so  $|\frac{\omega}{\omega_c}| - 1 = 1.16$ .

To get more than 30dB attenuation, a 3dB equal-ripple filter of  $N = 3$  is needed so from the table in the appendix, it is known that  $g_1 = 3.3487 = L_1$ ,  $g_2 = 0.7117 = C_2$ ,  $g_3 = 3.3487 = L_3$  and  $g_4 = 1$ .

After scaling the values will be  $L_1 = 251.1675$ ,  $C_2 = 0.00949$ ,  $L_3 = 251.1675$  and  $g_4 = 75$ .

After the order ( $n$ ) of the prototype has been decided, we construct the circuit of the low-pass filter prototype. The figure below shows the circuit diagram of a third order low pass filter prototype. The prototype that begins with the series element was chosen. Figure 3.3 shows the circuit diagram of the low pass prototype beginning with a series element. The element values for Equal-Ripple low-pass filter prototype is shown on the table in the appendix. For a third order prototype, the values will be  $g_1 = 3.3487 = L_1$ ,  $g_2 = 0.7117 = C_2$ ,  $g_3 = 3.3487 = L_3$  and  $g_4 = 1$ .

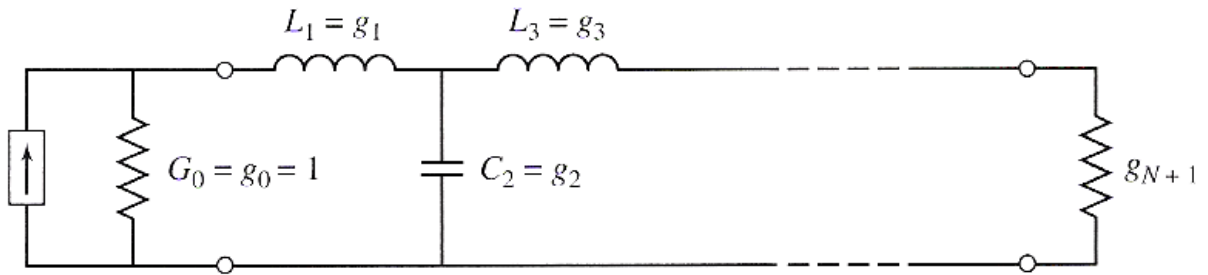


Figure 3.3: Prototype beginning with a series element [9].

From the above theory of transformations,

$$\Delta = \frac{\omega_2 - \omega_1}{\omega_0} = \frac{2\pi(93.5\text{MHz} - 82.5\text{MHz})}{2\pi(\sqrt{(82.5\text{MHz})(93.5\text{MHz})})} = 0.125.$$

For series inductor  $L'_k$ , the series LC circuit with element values

$$L'_k = \frac{L_k}{\Delta\omega_0} = \frac{251.15}{(0.125)(2\pi(87.827\text{MHz}))} = 3.64\mu\text{H}$$

$$C'_k = \frac{\Delta}{\omega_0 L_k} = \frac{0.125}{(2\pi(87.827\text{MHz}))(251.15)} = 0.9\text{pF}$$

For shunt capacitor  $C_k$ , the shunt LC circuit with element values

$$L'_k = \frac{\Delta}{\omega_0 C_k} = \frac{0.125}{(2\pi(87.827\text{MHz}))(0.00949)} = 23.87\text{nH}$$

$$C'_k = \frac{C_k}{\Delta\omega_0} = \frac{0.00949}{(0.125)(2\pi(87.827\text{MHz}))} = 137.5\text{pF}$$

These component values were checked with a software called Ansoft Designer SV. This program can easily design a bandpass filter with the specifications one requires. Figure 3.4 below shows the filter response and the circuit diagram designed by Ansoft Designer SV.

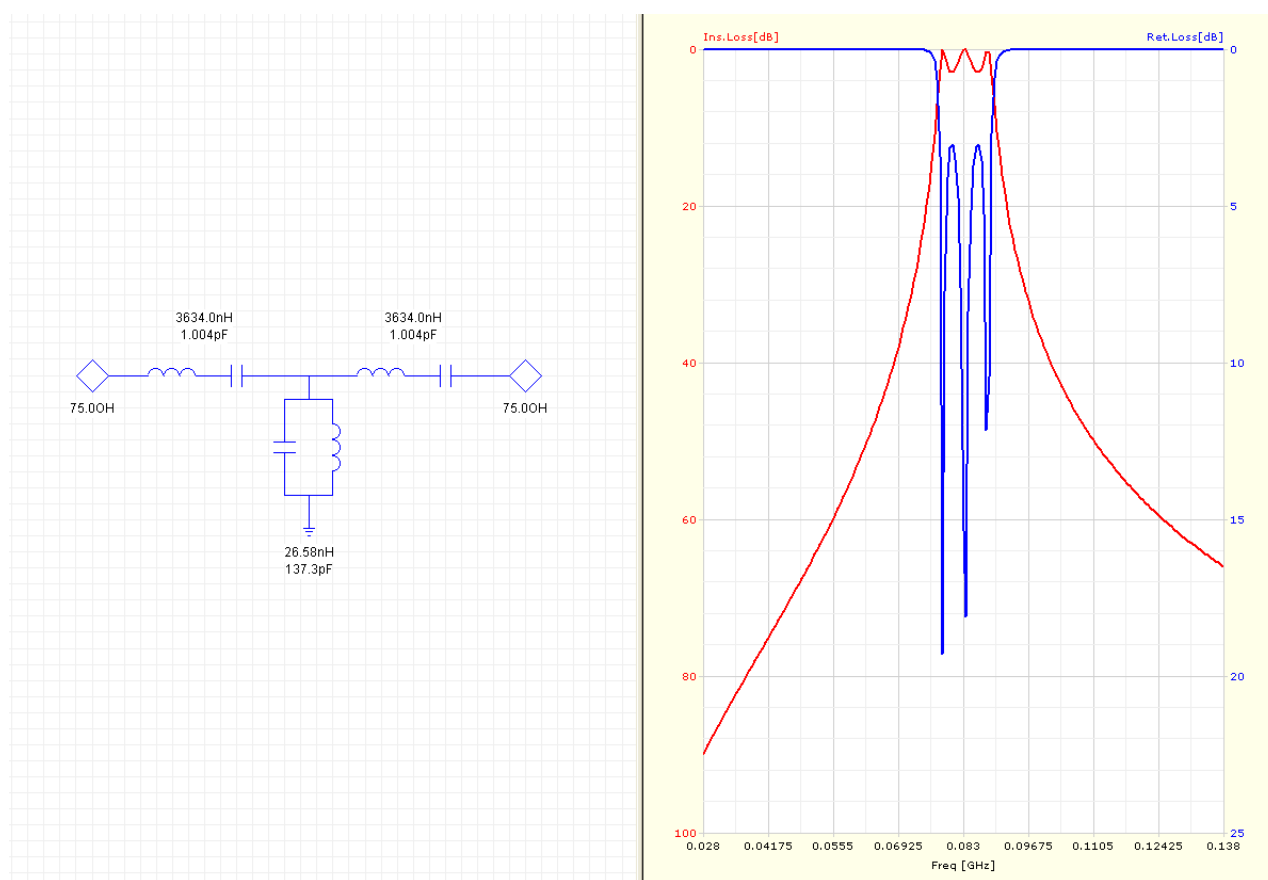


Figure 3.4: Ansoft produced frequency response

### 3.2.4 Construction

#### Picking component values

At this stage of the design process, many problems arose due to the component values, that was needed for the filter, not being realisable (i.e. doesn't come in standard component values). The closest values were  $3.3\mu H$ ,  $3.9\mu H$ ,  $100pF$ ,  $1pF$  respectively. There was no component value that came close to  $23.87nH$  provided in the university labs and due to time limitations, we could not order them from the suppliers.

Initially, the  $3.3\mu H$ ,  $100pF$ ,  $1pF$  was decided to construct the filter and to test the response. The other inductor was decided to be constructed by winding. Each component was tested separately to check if it can perform at the right values from the network analyser. Our focus was at the bandwidth of 82.5MHz to 93.5MHz.

After testing, it was found that the  $3.3\mu H$  and the  $3.9\mu H$  inductors did not work because at high frequencies, the inductors will have a capacitive response, the inductor will act (transform to act) like a inductor connecting in parallel with the capacitor. The  $100pF$  capacitor at around 88MHz turn out to have a component value of  $138pF$  response, so it was ideal for our design. The  $1pF$  capacitor drove up to  $2pF$  at 88MHz. It was decided that one should construct the capacitor with two  $1pF$  capacitors connecting them in series. This will have a  $1pF$  ( $\frac{1}{C_{tot}} = \frac{1}{C_1} + \frac{1}{C_2}$ ) response. But not all components values are manufactured perfectly so each component values need to be tested.

After testing the components, both inductor values were decided to be winded by hand. In theory , the inductance of an N turn coil is  $N^2$  times that of a single turn, i.e.

$$L = N^2 \mu r [\ln(\frac{8r}{a}) - 2],$$

where  $r$  is the radius of the winding (circle),  $a$  is the radius of the wire (coil) and  $\mu = \mu_r \mu_0$ , but  $\mu = \mu_0$  in copper.

so

$$N = \sqrt{\frac{L}{\mu r [\ln(\frac{8r}{a}) - 2]}} = \sqrt{\frac{23.87nH}{(4\pi \times 10^{-7})(0.0015)(\ln(\frac{8(0.0015)}{0.0004}) - 2)}} = 3$$

and

$$N = \sqrt{\frac{L}{\mu r [\ln(\frac{8r}{a}) - 2]}} = \sqrt{\frac{3.64 \times 10^{-6}}{(4\pi \times 10^{-7})(0.004)(\ln(\frac{8(0.004)}{0.0004}) - 2)}} = 17.44 \approx 18$$

This is how the inductors were winded. Both inductors were tested after winding and it worked with  $N = 24$  for the  $3.64\mu H$  inductor because 18 turns turned out to be too small in value. The  $N = 3$  for the  $23.87nH$  inductor with a different  $r$  was used at 88.2MHz. Figure 3.5 shows the response

of the  $23.87nH$  inductor on the smith chart. The inductance varies with the change in frequency as indicated with yellow on the smith chart.

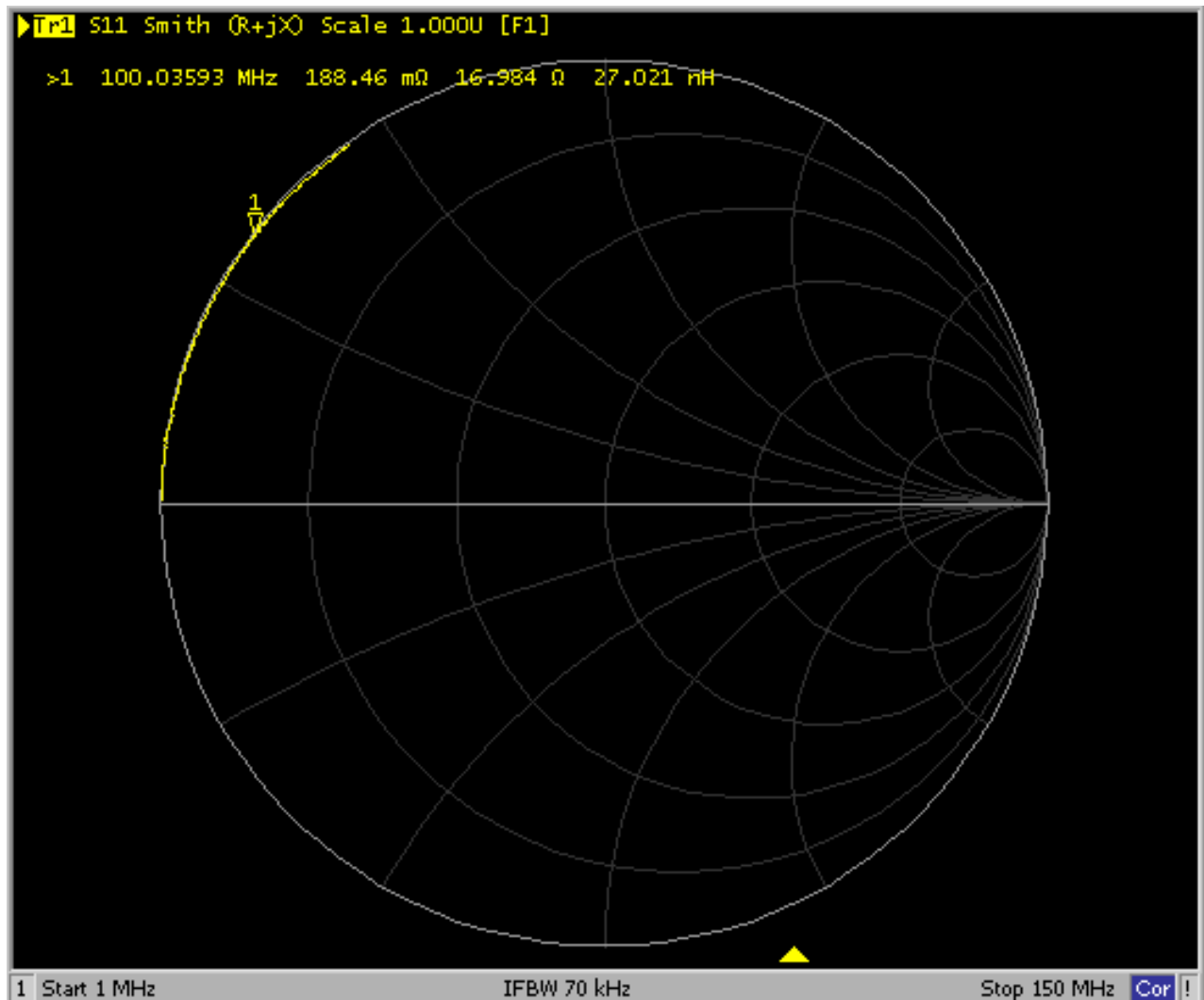


Figure 3.5: Inductance at 100MHz on the smith chart.

### Actual construction and testing

After all the component values were decided, the construction began with drilling holes on the boards for the components and BNC connectors. The components and the connectors were fitted in and soldered into place. After the bandpass filter was constructed, it was tested with a network analyser and the responses weren't up to specification.

### Final results

The two  $1pF$  capacitor were taken off knowing that there is capacitance existing between the coils of the inductors at high frequencies. After removing the two  $1pF$  capacitors on the series LC circuit,

it was tested again on the network analyser and it worked almost perfectly. Centred at 88.2MHz and 20dB attenuation at 96MHz. Figure 3.7 show the frequency response and the attenuation of the bandpass filter. Figure 3.6 shows the 3dB bandwidth of the filter.

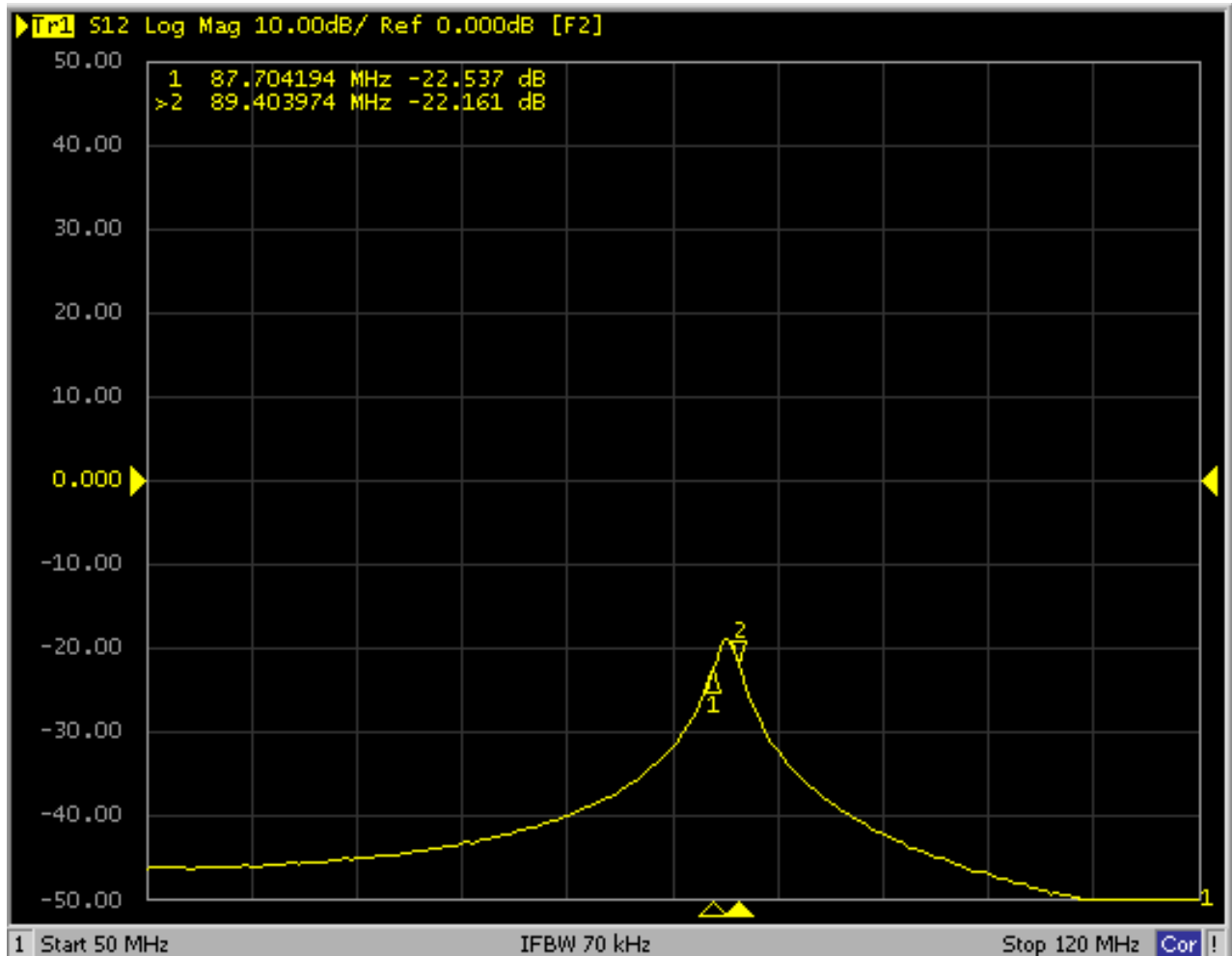


Figure 3.6: 3dB bandwidth of the filter

The main problems that were found in the designs of these filters was that the wires were too lossy at high frequencies. Without winding the wires, the wires has a -3dB loss at around 94MHz. Figure 3.8 show the wire losses at 94MHz. If the wires are wound to become an inductor. The losses due to the winding will be -10dBs at around 88MHz. Figure 3.9 shows the coil losses at 88MHz. Although the filters have high losses, it can be compensated with proper amplifiers.

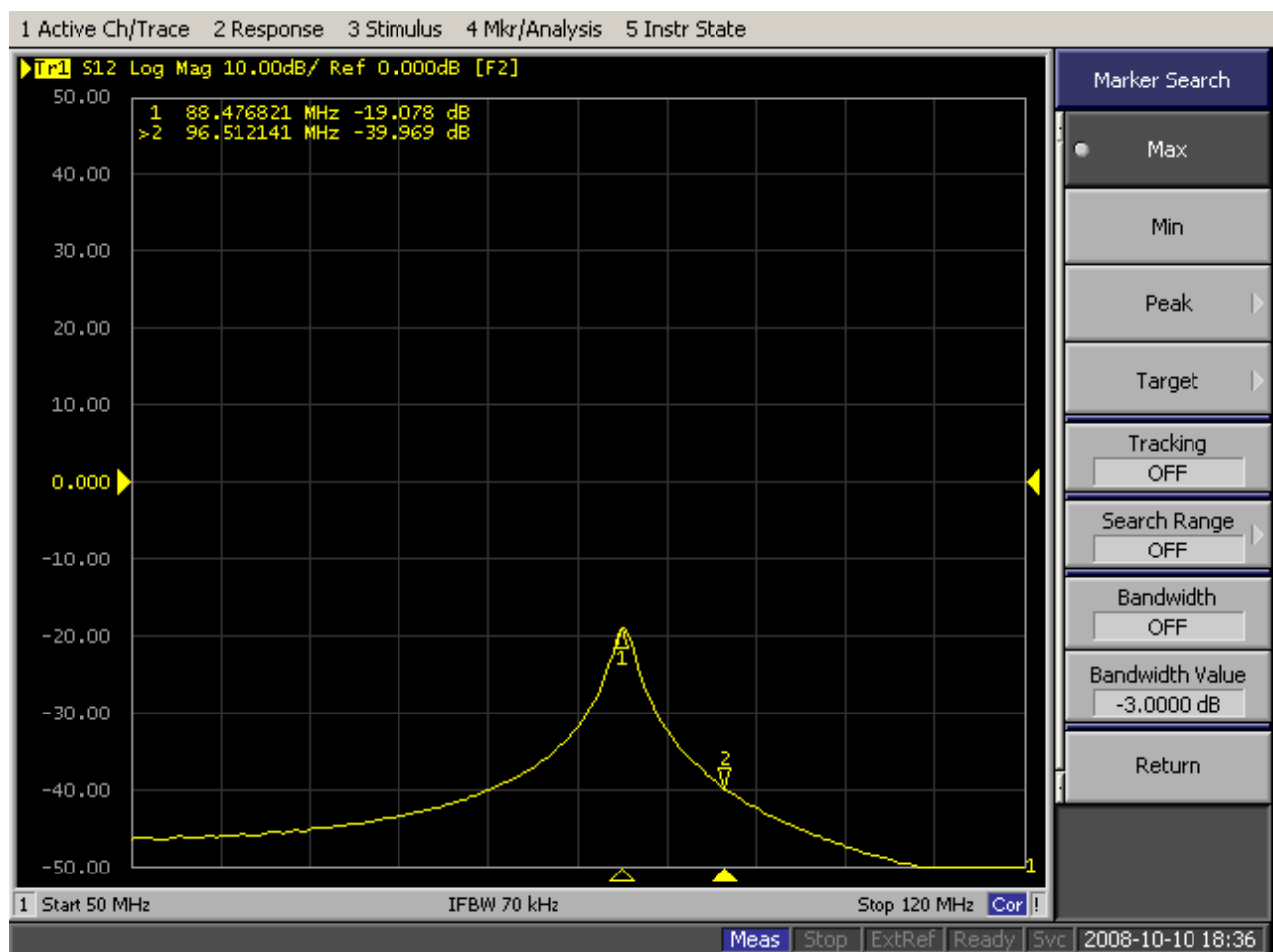


Figure 3.7: Filter response attenuation.



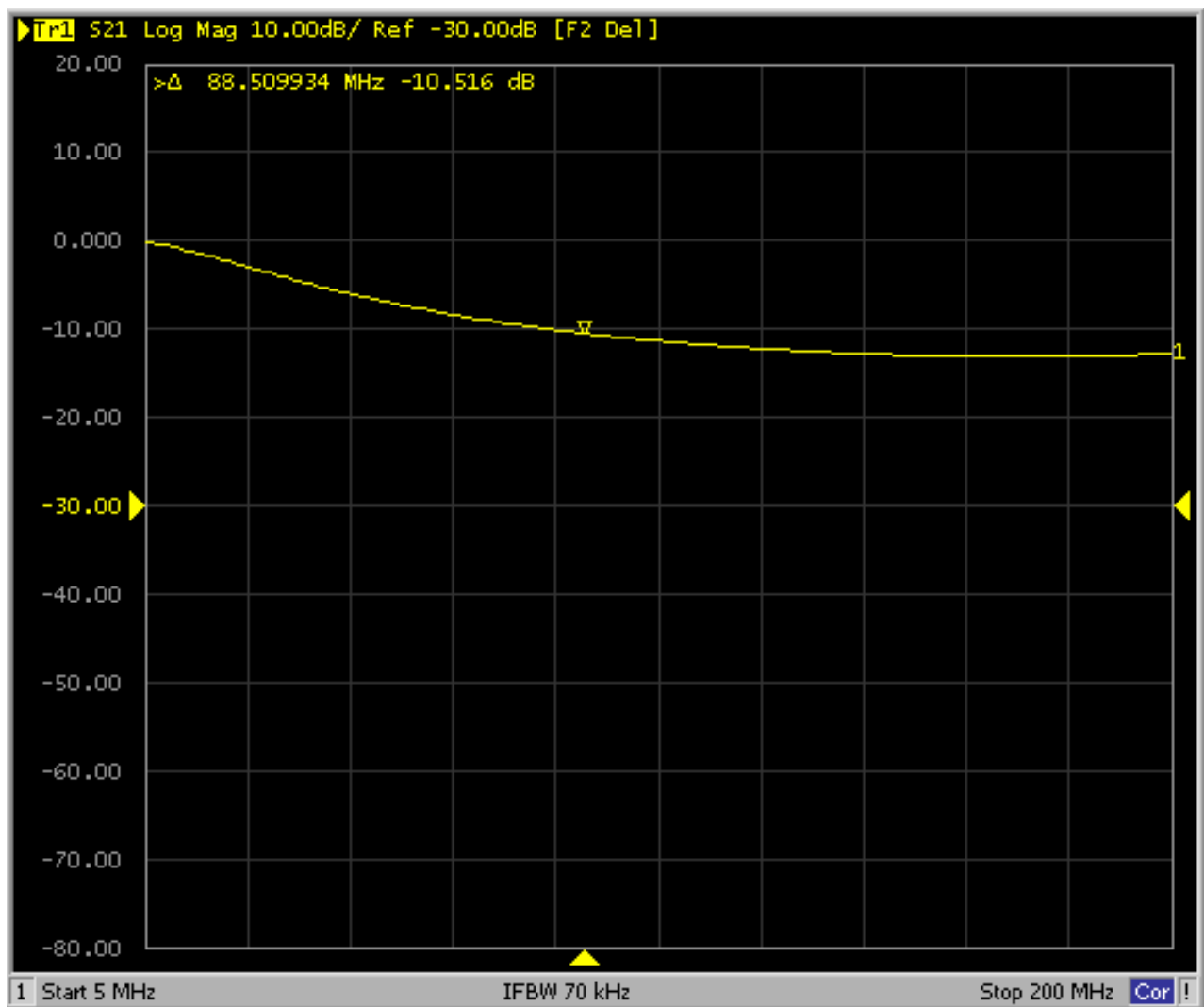


Figure 3.9: Resonance frequency of a inductor (winded wire)

# Chapter 4

## Simulations

### 4.1 Pre-setup

#### **FERS**

Flexible, Extensible Radar and Sonar simulator (FERS) is a multistatic radar simulator written by Marc Brooker for a PhD student in the electrical engineering department.

A program (in FERS) was written by a postgraduate student (Sebastiaan Heunis) from the University of Cape Town is used in this section to simulate a radar configuration consisting of one transmitter, receivers and moving targets. In the program, some codes needed to be modified to meet our requirements in order to perform the different techniques. Our main focus is to locate the angle of arrival from the transmitter to the receiver(s).

In this research, the objective was to find the angle of arrival for a FM signal (around 79 - 109MHz), so 100MHz is picked for simplicity of calculations. A MP3 called 'killswitch.mp3' was converted and used as a signal for our research. The MP3s sampling frequency is at 44.1kHz but when we work with FM signals, it will be ten times the normal sampling frequency. So the sampling frequency will be at 441kHz and both carrier and clock frequency is set to 100MHz.

The transmitter that was used is the Tygerberg station in Platterkloof. The coordinate system of the Tygerberg station with respect to UCT at (0,0) is (12353,9613). After all of this were set, the simulations could begin.

## 4.2 Simulation setup

The FM signal of 100MHz is used, so the wavelength  $\lambda = \frac{c}{f} = \frac{3 \times 10^8}{1 \times 10^8} = 3m$ . The Linear resolution of the FM signal  $\delta = \frac{c}{2B} = \frac{3 \times 10^8}{2 \times 100kHz} = 1500m = 1.5km$ . The angular resolution will be  $\Delta = \frac{\lambda R}{2D} = \frac{\lambda}{2 \sin \theta} = \frac{cR}{2DF}$ . Co-ordinate of transmitter  $\rightarrow (12353, 9613)$ . Angle of arrival from Tygerberg to UCT is  $37.89^\circ$ .

### 4.2.1 Interferometer

According to the background of interferometer technique that was discussed in chapter 2, the distance  $d$  between the antennas in the antenna array must be less or equal to  $\frac{\lambda}{2}$  to prevent ambiguity. A value of  $0.4\lambda$  is taken with a appropriate 20% margin to  $0.5\lambda$ , so  $d = 0.4(3m) = 1.2m$ . For a better angular resolution, an array of four antennas were used, each of them separated by  $1.2m$ . The angular resolution  $\Delta = \frac{3 \times 15652.7}{2 \times 3.6} \approx 6522m$ . In FERS, the transmitter position was set to (12353,9613). Many receivers were created to make an array of antennas. Using UCT as a reference, the receivers were positioned at (0.0,0.0), (1.2,0.0), (2.4,0.0) and (3.6,0.0) respectively. The amplitude is set to zero (only interested in two dimensions). After all the codes have been modified, the simulation could begin.

By compiling the program that was modified, FERS will create many files and it includes the signals of interest. Four received signals were created in a 'h5' format and by using the 'h5import.m' matlab function, the signals could be processed to find the angle of arrival. It has been later found out that in the program given, the results (including phase) of the four received signals has also been generated after compiling the FERS program. The results include the phase of all four signals that were required to find the angle of arrival.

### 4.2.2 Triangulation

The setup in FERS for triangulation is almost the same as the interferometer. The only difference is that the coordinates of the receivers must be modified. The triangulation technique used in this simulation is the time difference of arrival method. When using this method, one must make sure that the distances (R) between transmitter to each receiver must not be the same or else the method will not work because there will be no time difference (delay). This method will also not work if the antennas are too close to each other because the resolution of a FM frequency is around 1.5km.

In this simulation, the position of the receivers were decided at (0,0), (15000,-15000), (13000,-8000) and (30000,30000) respectively. The distance from transmitter to receivers are approximately 15,20

and 40km. The receivers must be far away from each other because of resolution of the signals. The further apart, the better the accuracy.

## 4.3 Results

### 4.3.1 Interferometer

The interferometer technique is implemented by the phase delay of the arrived signals. From compiling the FERS program, the phase of the signal will appear in the result files. The phase of the signals are as follows:

- Signal 1 (0.0,0.0):  $1.08008 (+2\pi) = 7.36326$
- Signal 2 (1.2,0.0): 5.37847
- Signal 3 (2.4,0.0): 3.39375
- Signal 4( 3.6,0.0): 1.40910

Figure 4.1 , 4.2 and 4.3 shows the phase difference of the signals. The first figure shows the zoomed out version of the phase difference of the signal which cannot be seen by the human eye. The other two figure shows a close up view of the phase difference of the signal.

So the change in phase between signals will be:

- $\Delta phase(sig1, sig2) = 1.98479$
- $\Delta phase(sig2, sig3) = 1.98472$
- $\Delta phase(sig3, sig4) = 1.98465$

So the *mean* of the change in phases is  $\Delta phase = \nabla \psi = 1.98472$ .

Apply the formula that was discussed in chapter 2,

$$\theta = \sin^{-1}\left(\frac{\lambda \nabla \phi}{d \times 2\pi}\right) = \sin^{-1}\left(\frac{3 \times 1.98472}{1.2 \times 2\pi}\right) = 52.157^\circ$$

But our angle of interest is the angle from east toward north, so

$$\theta = \cos^{-1}\left(\frac{\lambda \nabla \phi}{d \times 2\pi}\right) = \cos^{-1}\left(\frac{3 \times 1.98472}{1.2 \times 2\pi}\right) = 37.843^\circ$$

The calculated angle of arrival is  $\theta = 37.89^\circ$ . This measurement is very accurate because the signal generated has very low noise. So the SNR is very big, that means that the phase error variance in equation 2.5 is very small.

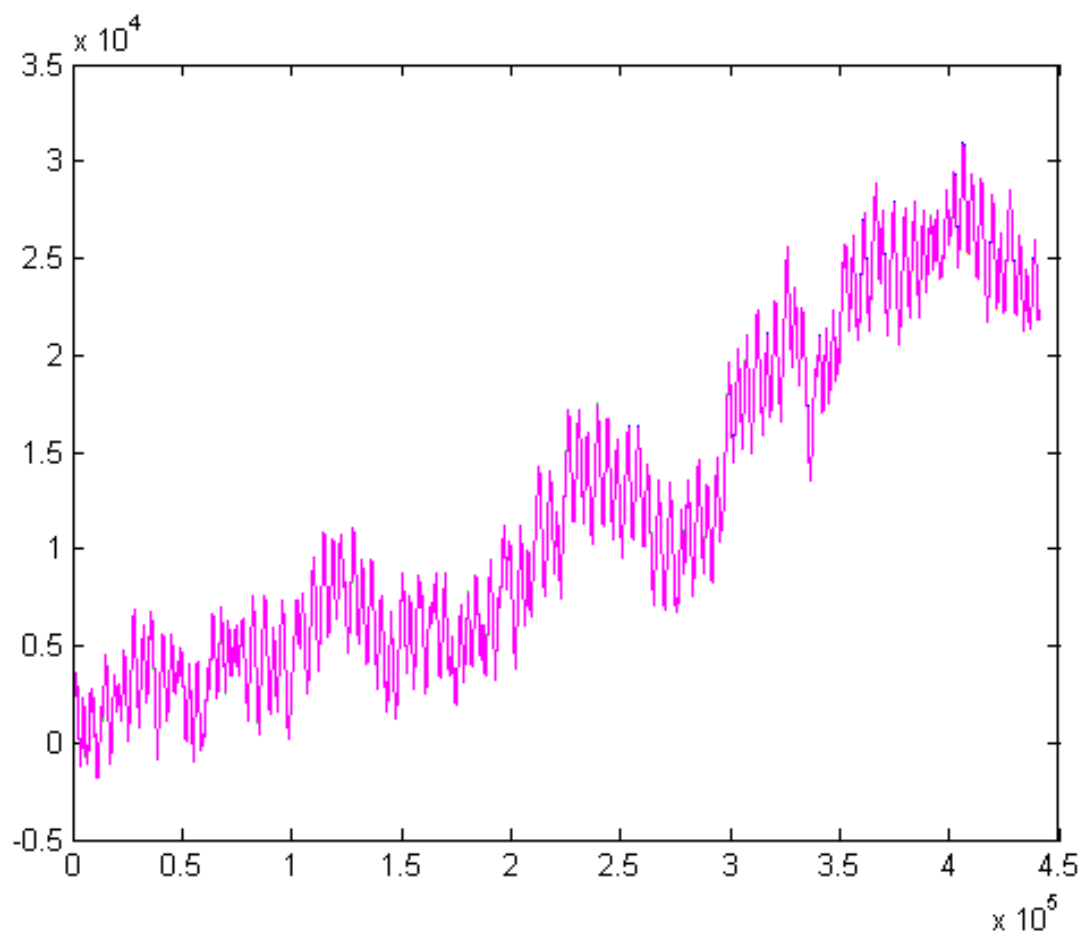


Figure 4.1: Phase difference zoomed out

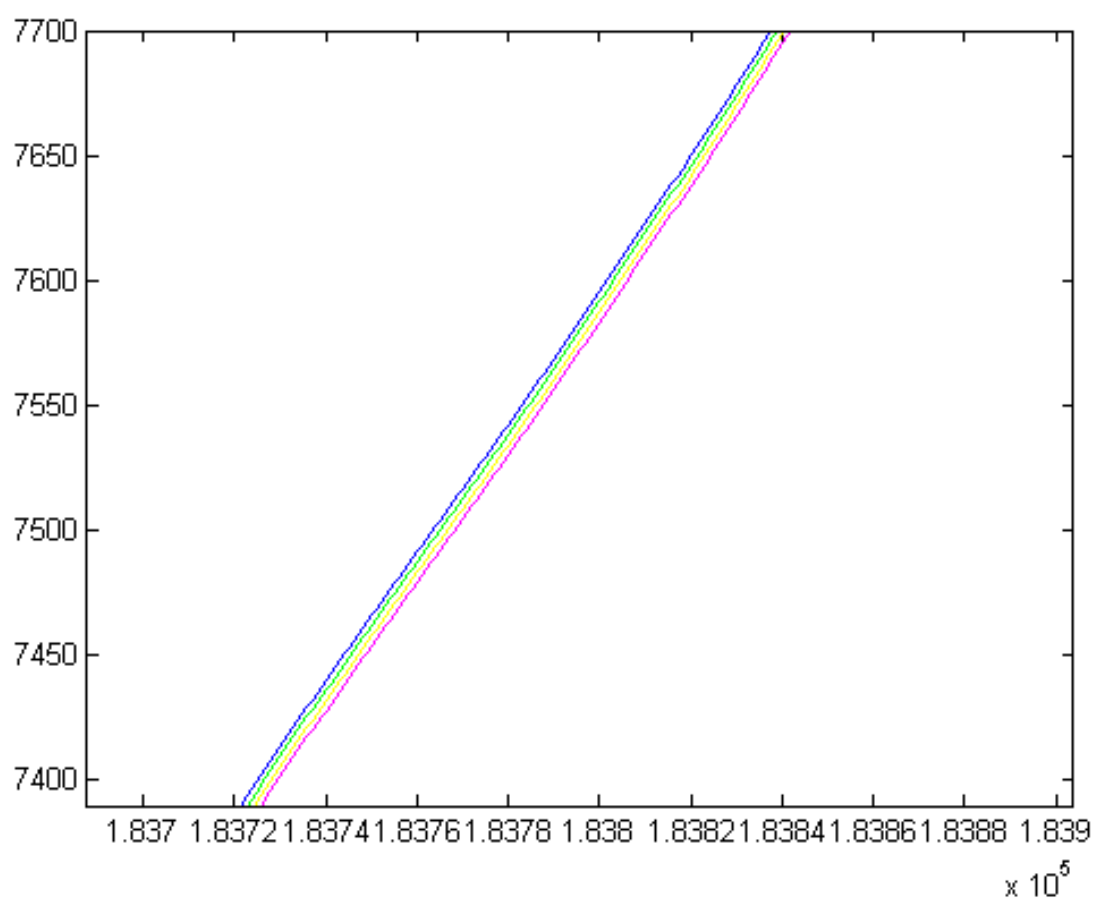


Figure 4.2: Phase difference zoomed in

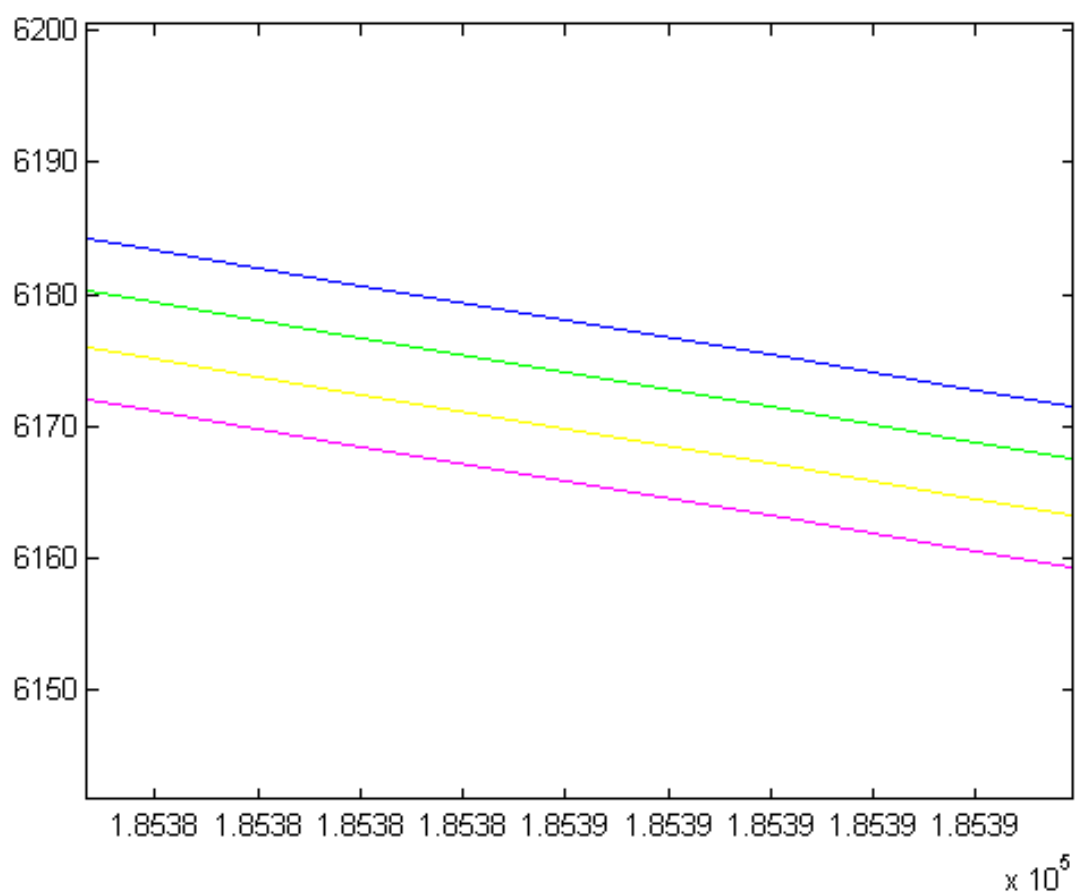


Figure 4.3: Close up view of phase difference

### 4.3.2 Triangulation

Triangulation technique uses the time difference of arrival method to find the target location and the angle of arrival. From compiling FERS, we can import the signals into MATLAB for further processing.

In MATLAB, we correlate signal 1 with signal 2, signal 1 with signal 3 and signal 1 with signal 4 respectively using the build in 'xcorr' function to get the time delay between the signals. Figure 4.4, 4.5 and 4.6 shows the time delay between the signals

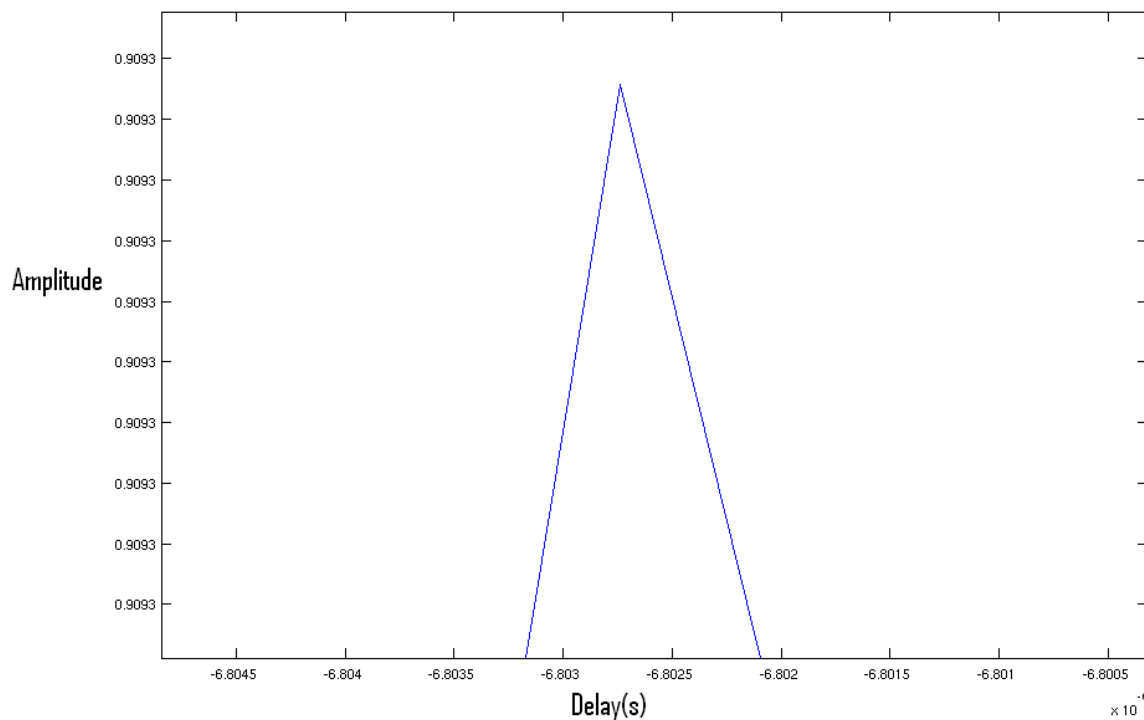


Figure 4.4: Signal one correlate with signal two

The built in 'max' function in MATLAB can locate the time delay (call it  $\tau_1$ ,  $\tau_2$  and  $\tau_3$ ) at maximum amplitude. By using the delay that is processed from the data, the variable  $R_{a0}$ ,  $R_{b0}$  and  $R_{c0}$  can be found by

$$R_{a0} = c \times \tau_1 = 3 \times 10^8 \times -6.8027 \times 10^{-6} = -2040.81$$

$$R_{b0} = c \times \tau_2 = 3 \times 10^8 \times -2.9479 \times 10^{-5} = -8843.7$$

$$R_{c0} = c \times \tau_3 = 3 \times 10^8 \times -3.8549 \times 10^{-5} = -11564.7$$

After the values of the variables  $R_{a0}$ ,  $R_{b0}$  and  $R_{c0}$  has been found, apply them to equation 2.3 or 2.4 to solve for the values of  $x$  and  $y$  which is the position of the transmitter. After finding the coordinates of the transmitter, the angle of arrival could simply be found by taking the gradient of the transmitter

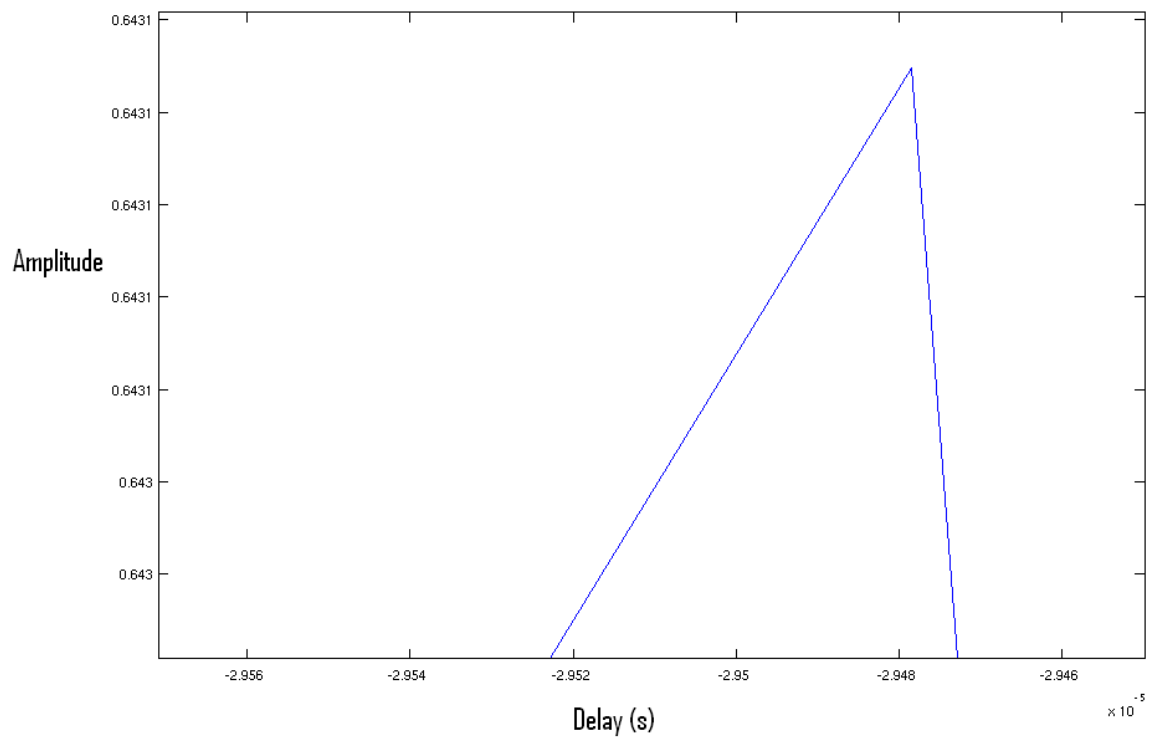


Figure 4.5: Signal one correlate with signal three

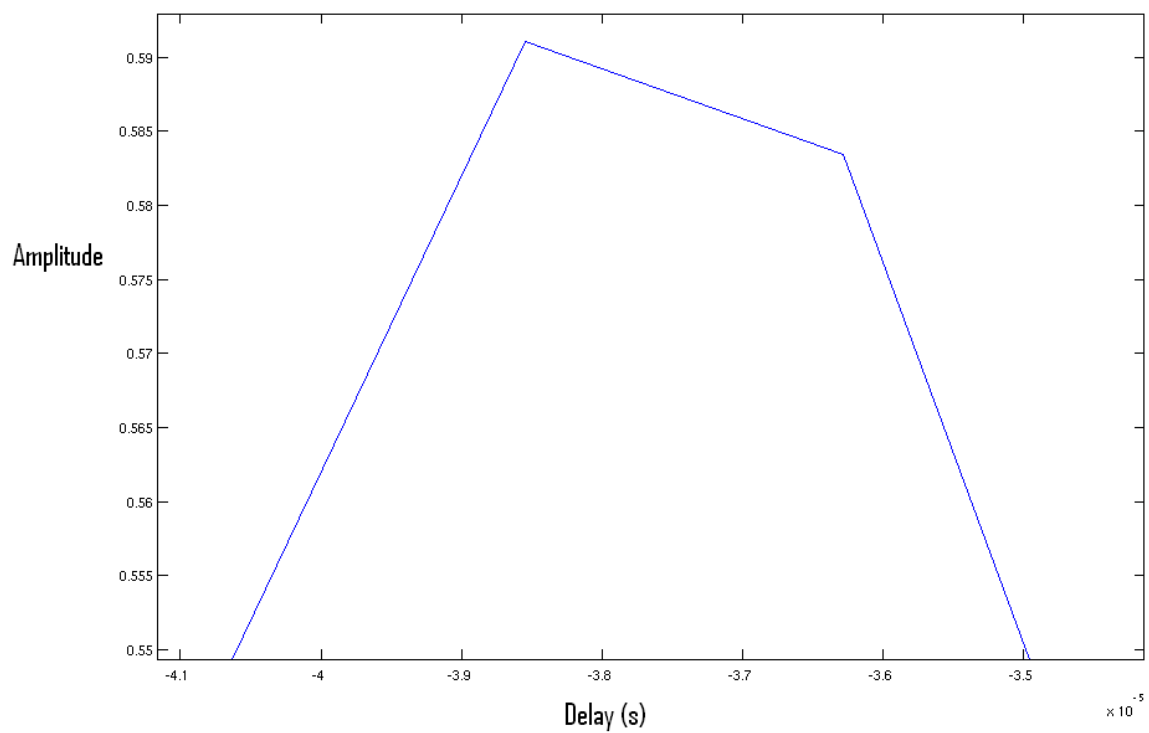


Figure 4.6: Signal one correlate with signal four

to each receiver. The gradient of the transmitter to receiver baseline can be expressed by

$$m = \tan\theta$$

where  $\theta$  is the angle from east counting anti-clockwise and  $\theta$  is given in radians. From basic trigonometry, if  $\tan\theta$  equals a negative number, the angle will be either at the 2nd or 4th quadrant and if  $\tan\theta$  is positive, it will lie in either 1st or 3rd quadrant. There is a problem to the solution because  $\tan\theta$  creates an ambiguity of  $180^\circ$  so one cannot distinguish between  $\theta$  and  $(180^\circ + \theta)$ . To solve this problem, the coordinate positions must be compared. This is all programmed in MATLAB. The code of this function is attached in the appendix.

Figure 4.7 shows the positions of the receivers in blue and the transmitter in green. The red cross indicate where the actual transmitter should be. Figure 4.8 shows the angle of arrival from the transmitter to the receivers.

## Results

Co-ordinates (x,y)  $\rightarrow$  (11965,9388)

Angle 1 (0,0)  $\rightarrow$  38.1189°

Angle 2 (13000,-8000)  $\rightarrow$  93.4073°

Angle 3 (15000,-15000)  $\rightarrow$  97.0944°

Angle 4 (30000,30000)  $\rightarrow$  228.8146°

### 4.3.3 Comparison

Both techniques has its advantages and disadvantages. The interferometer techniques give an accurate angle of arrival information that gives an angular accuracy of around  $0.05^\circ$  but this technique can only find the angle of arrival information. Interferometer technique cannot locate the position of the transmitter because the array of antennas are too close to each other (1.2m). Antenna arrays used for interferometry can not locate the co-ordinates of the transmitter by triangulation because of the poor range resolution. The distance between the antennas are not sufficient enough to the resolution of FM signals (1.5km).

On the other hand, time difference of arrival (or triangulation) technique has a poorer angular accuracy than the interferometer technique. The angle of arrival from the Tygerberg transmitter to UCT obtained by simulation is  $38.12^\circ$ , but the theoretical angle of arrival is supposed to be  $37.89^\circ$ . The accuracy is around  $0.25^\circ$  which is poorer than the interferometry ( $0.05^\circ$ ). Comparing the position determined by simulation to the theoretical value, it is found that the position of the transmitter is (11965,9388) but the theoretical position is (12353,9613) which is very accurate considering the

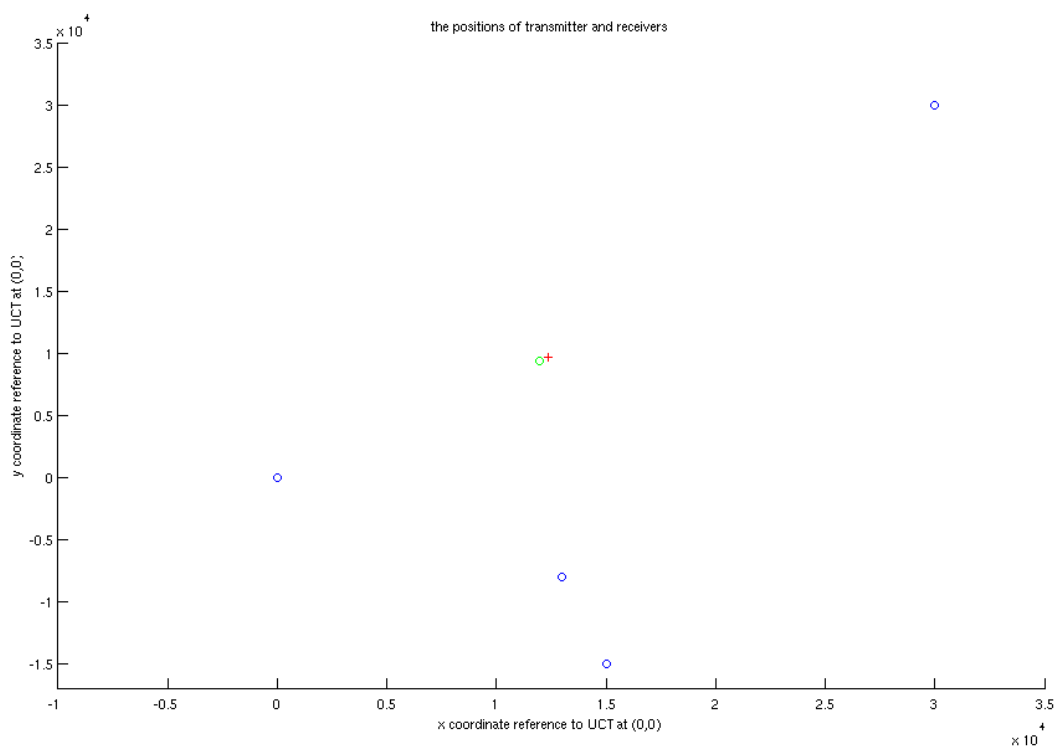


Figure 4.7: Positions of the transmitter and the receivers

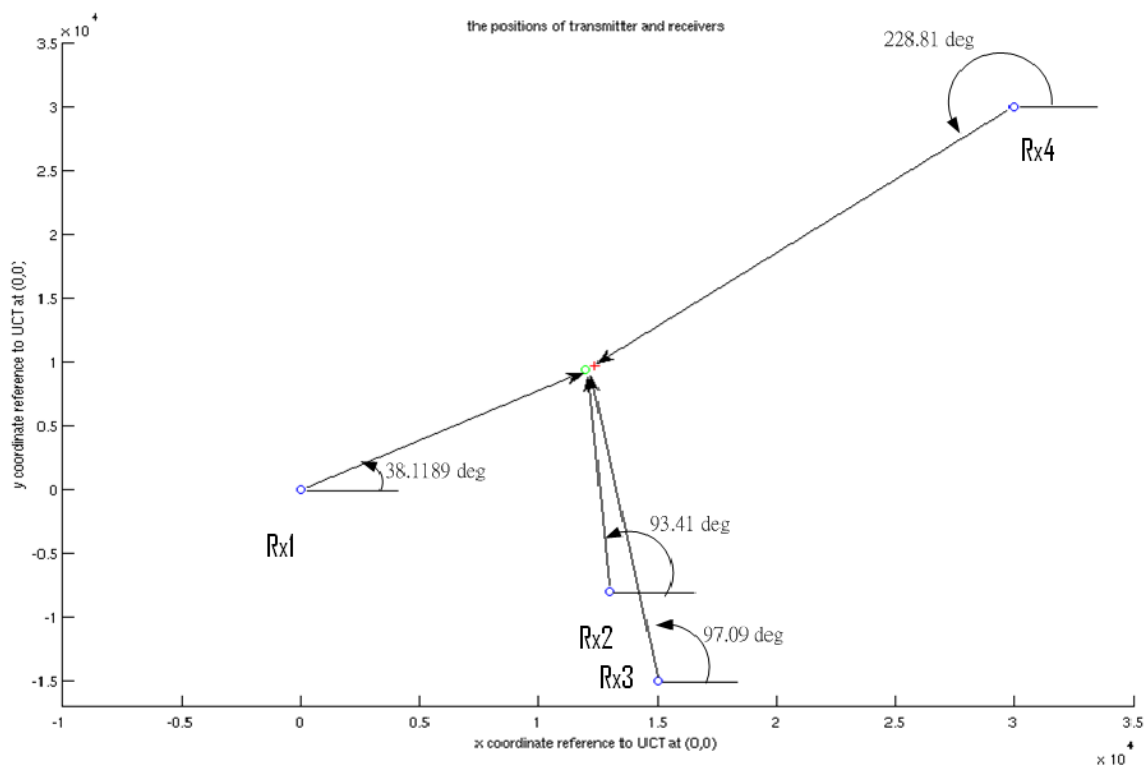


Figure 4.8: Position of the transmitter and the receivers with the angle of arrival

resolution of the signal. Although this technique is less accurate than the angular accuracy of the interferometer technique, but it can locate the position of the transmitter.

# Chapter 5

## Experimentation

### 5.1 Pre-Setup of interferometer

#### 5.1.1 USRP

The Universal Software Radio Peripheral (USRP) is a data acquisition board containing several distinct sections. The analog interface portion contains four analog to digital converter (ADC) and four digital to analog converter (DAC). The ADC's operate at 64 million samples per second (Msps) and the DAC's operate at 128 Msps. Since the USB bus operates at a maximum rate of 480 million million bits per second, the FPGA must reduce the sample rate in the receive path and increase the sample rate in the transmit path to match the sample rates between the high speed data converter and the lower speeds supported by the USB connection [8].

The AD9862 provides several functions. Each received section contains four ADC's. Before the ADC's there are programmable gain amplifiers (PGA) available to adjust the input signal level in order to maximise use of the ADC's dynamic range. The transmit path provides an interpolator and up-converter to match the output sample rate to the DAC sample rate and convert the baseband input to a low IF output. There are PGA's after the DAC's [8].

Most of the received signal processing is performed in the FPGA. First the signal is coupled into the AD9862. This chip contains two channels of ADC's and two channels of DAC's. The clock provided by the USRP drives the ADC's at 64 Msps. If needed, the AD9862 may divide this clock by two to reduce the sample rate. This only effects the clock rate of ADC's most of the sample rate conversion is done in the FPGA [8].

After the signal is digitised, the data is sent to the FPGA. The standard FPGA firmware provides two Digital Downconverters (DDC). The FPGA uses a multiplexer to connect the input streams from

each of the ADC's to the inputs of the DDC's. This multiplexer allows the USRP to support both real and complex input signals. The DDC's operate as real downconverters using the data from one ADC fed into the real channel or as complex DDC's where the data from one ADC is fed to the real channel and the data from another ADC is fed to the complex channel via the multiplexer [8].

The DDC consists of a numerically controlled oscillator, a digital mixer, and a cascade integrate comb (CIC) filter. These components down convert the desired channel to baseband (or low IF), reduce the sample rate and provide low pass filtering. For this research project, 64 decimation rate is used [8].

### 5.1.2 GNU-Radio

GNU Radio is an open source software toolkit. It supports Linux, MAC and windows machines. This software creates signal processing applications. It defines and process the waveforms in software. Computer programming skills, fundamentals of communication systems, digital signal processing are pre-requisites of using this software [6].

This software radio is an implementation technology. It is a technique for moving digital signal processing as close as possible to the antenna. Software radio is defined as “ *A radio that includes a transmitter in which the operating parameters of the transmitter, including the frequency range, modulation type or maximum radiated or conducted output power can be altered by making a change in software without making any hardware changes.*” [6]

#### A 3 tier architecture

Python scripting language is used for creating “signal flow graphs” and C++ is used for creating signal processing blocks. The scheduler is using Python's built-in module threading, to control the 'starting', 'stopping' or 'waiting' operations of the signal flow graph [6].

## 5.2 Interferometer design

For the purpose of this experiment, the 5FM (88.2MHz) signal was chosen. So the wavelength of the signal will be 3.4m.

### 5.2.1 Antenna

The Antenna used in this research is directive FM antennas. Two FM antennas were used in this experiment because of the limited space and resources for the experimentation. A structure for the

antenna was setup on the roof of the building. After setting up the structure, the antennas were attached 1.36m away from one another. The antenna was placed parallel to each other to act as an array. The received power from the antenna is -22dBm.

### 5.2.2 Amplifier

Two amplifiers were attached close to the antenna because the further it is from the antenna, the more noise will occur in the signal (The cable will create losses and noise). The amplifiers of each channel must be attached at the same distance from the antenna, so the cables must be the same length at any position along the system. The amplifier gain is 20dB.

### 5.2.3 Filter

The filter design was discussed in Chapter 3. The filter was attached at the end of the cable just before connecting it on the receiver (USRP). The cable from the amplifier to the USRP must be exactly the same length or else it will create a phase shift. At the other end of the filter, a 75 – 50 $\Omega$  converter was attached because the cable and the antenna are both 75 $\Omega$  but the USRP boards are 50 $\Omega$ , so the converter is used for matching. But the converters have around 6dB loss in each of them. The total loss from the filter is -20dB.

### 5.2.4 Receiver

The receiver used in this experiment is the USRP board which is connected to the filter from the input and into the computer as output. Two basic RX daughter boards were used for this experiment. It was attached to the receiver channel of the USRP board. Figure shows the setting up of the Interferometer system.

## 5.3 Testing

The received signals were tested before the experiment began. Figure 5.1, 5.2, 5.3 and 5.4 shows the response of antenna 1. Figure 5.5, 5.6 and 5.7 shows the response after adding an amplifier.

Figure 5.8, 5.9, 5.10 and 5.11 shows the response of the received signal from antenna 2. Figure 5.12, 5.13 and 5.14 shows the response after adding an amplifier.

### Results

Antenna 1 (with filter):

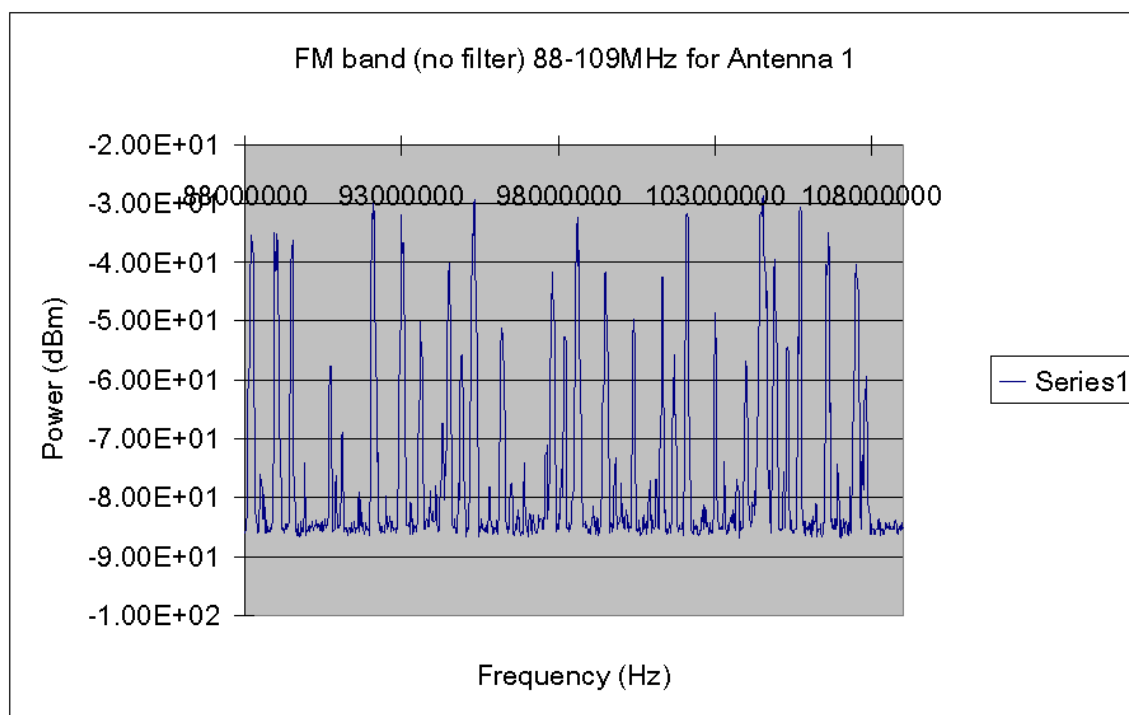


Figure 5.1: FM band

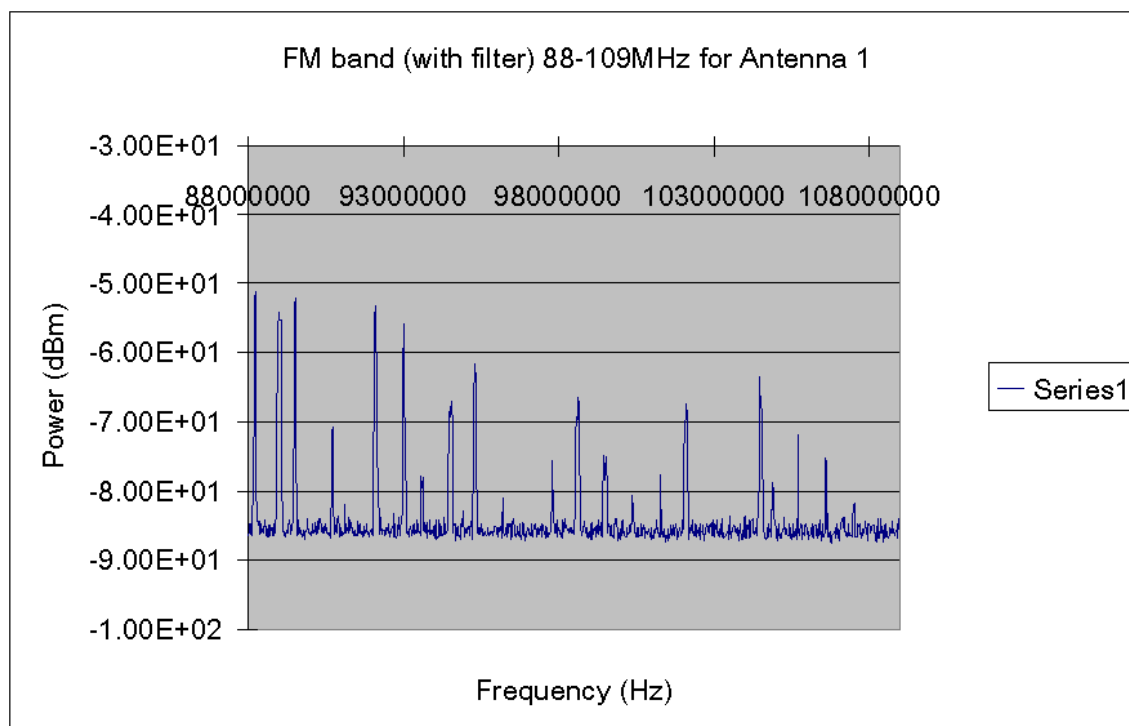


Figure 5.2: FM band with filter

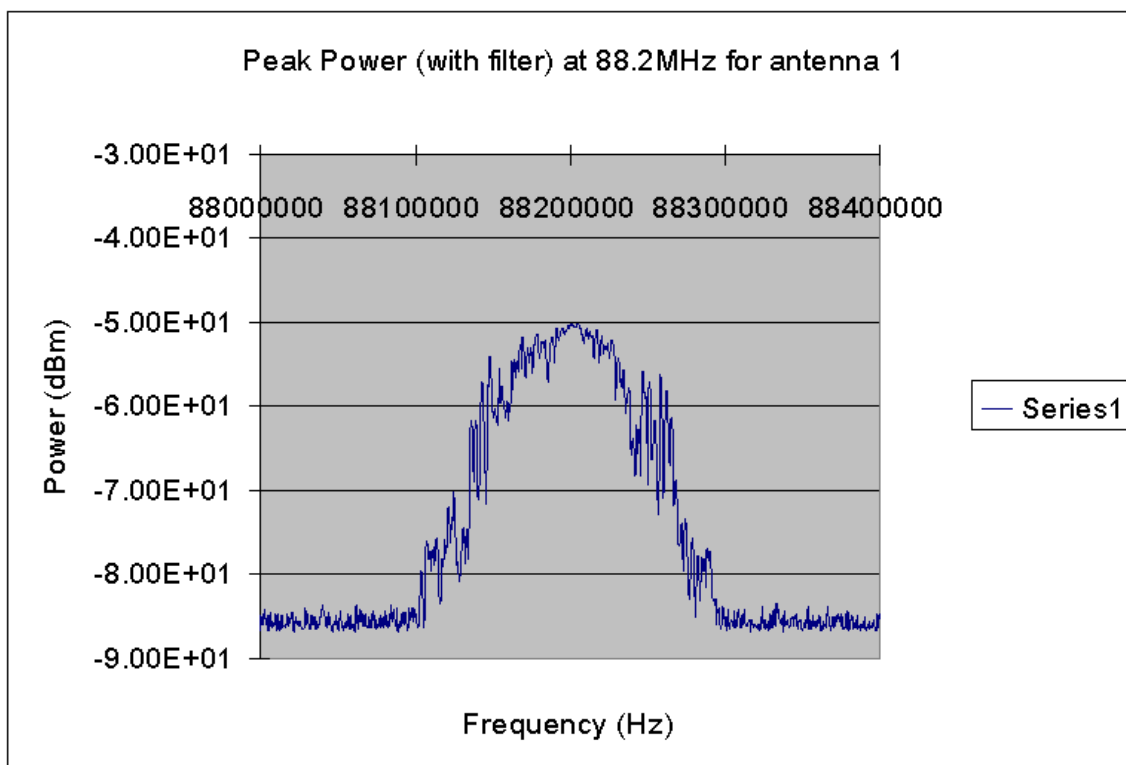


Figure 5.3: Peak Power at 88.2MHz

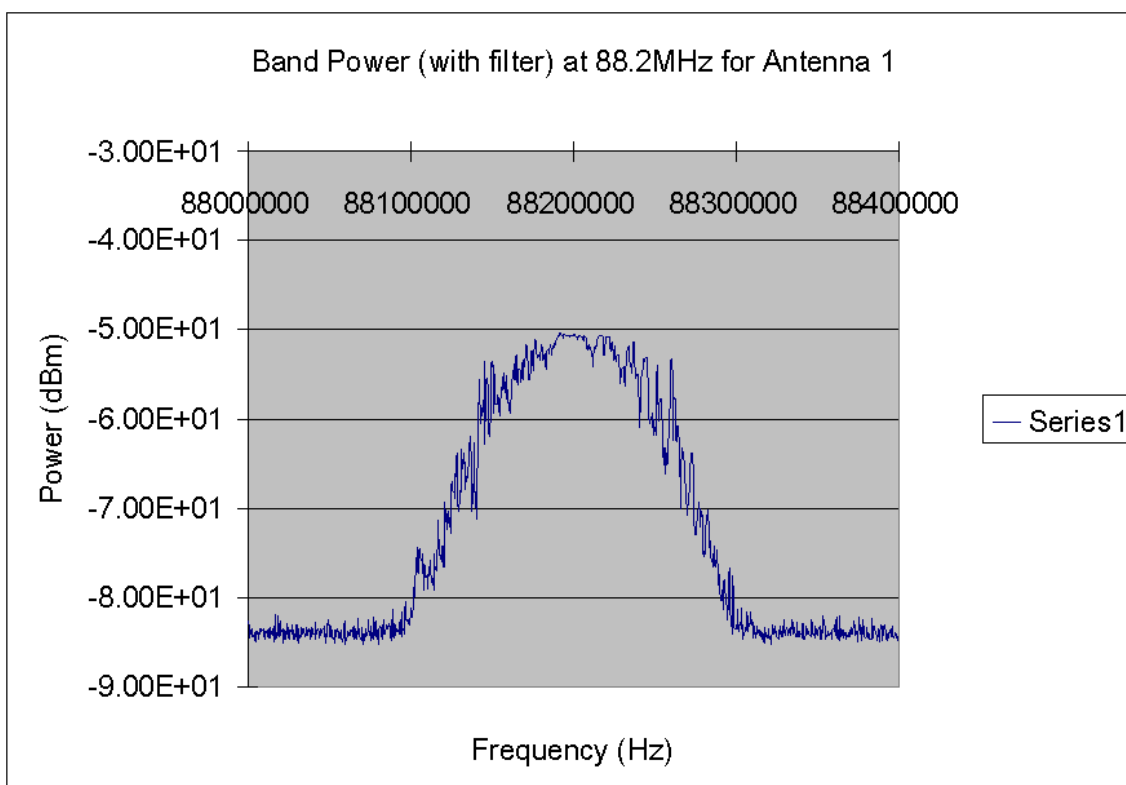


Figure 5.4: Band Power at centred at 88.2MHz

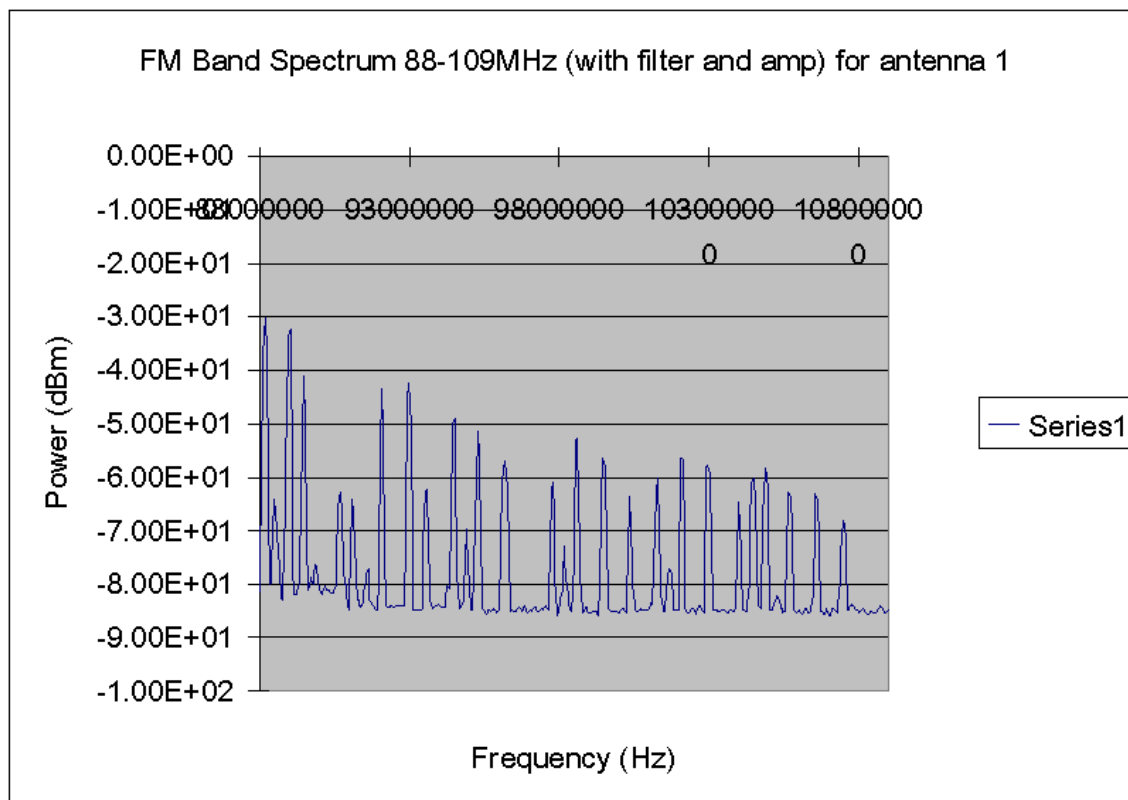


Figure 5.5: FM band (with amplifier)

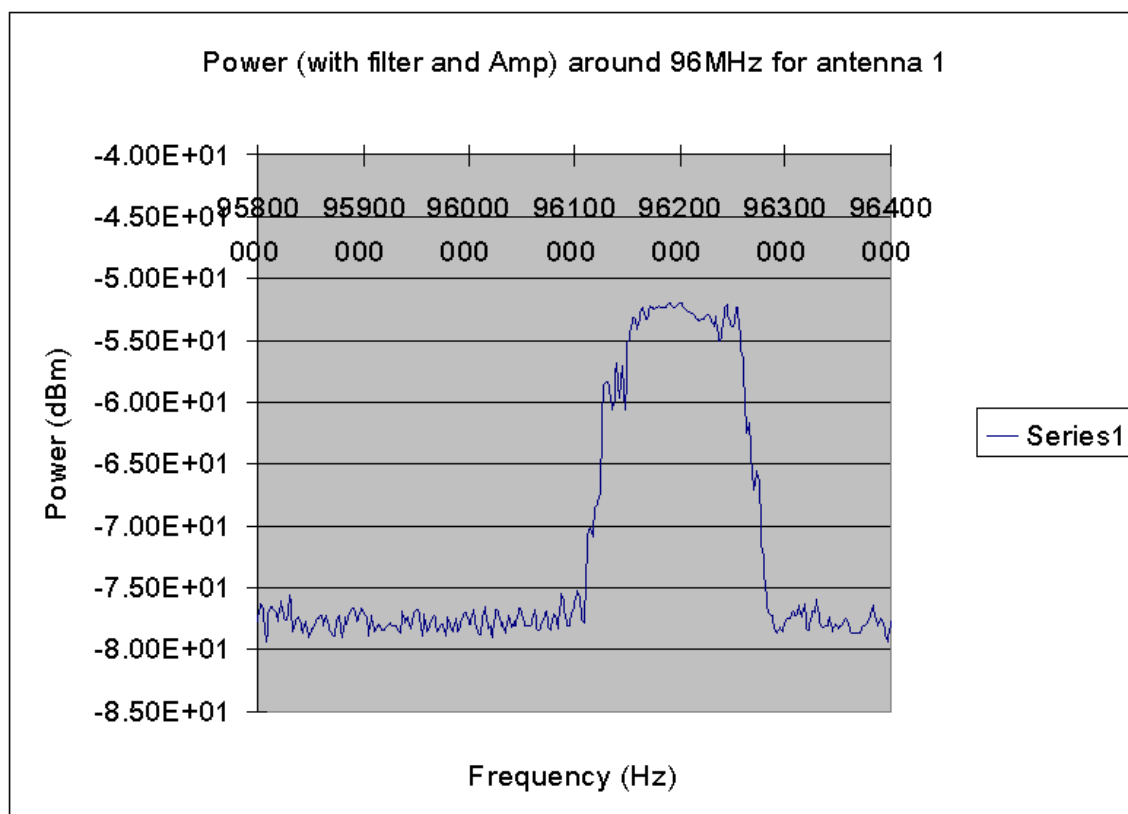


Figure 5.6: Peak power at 96MHz

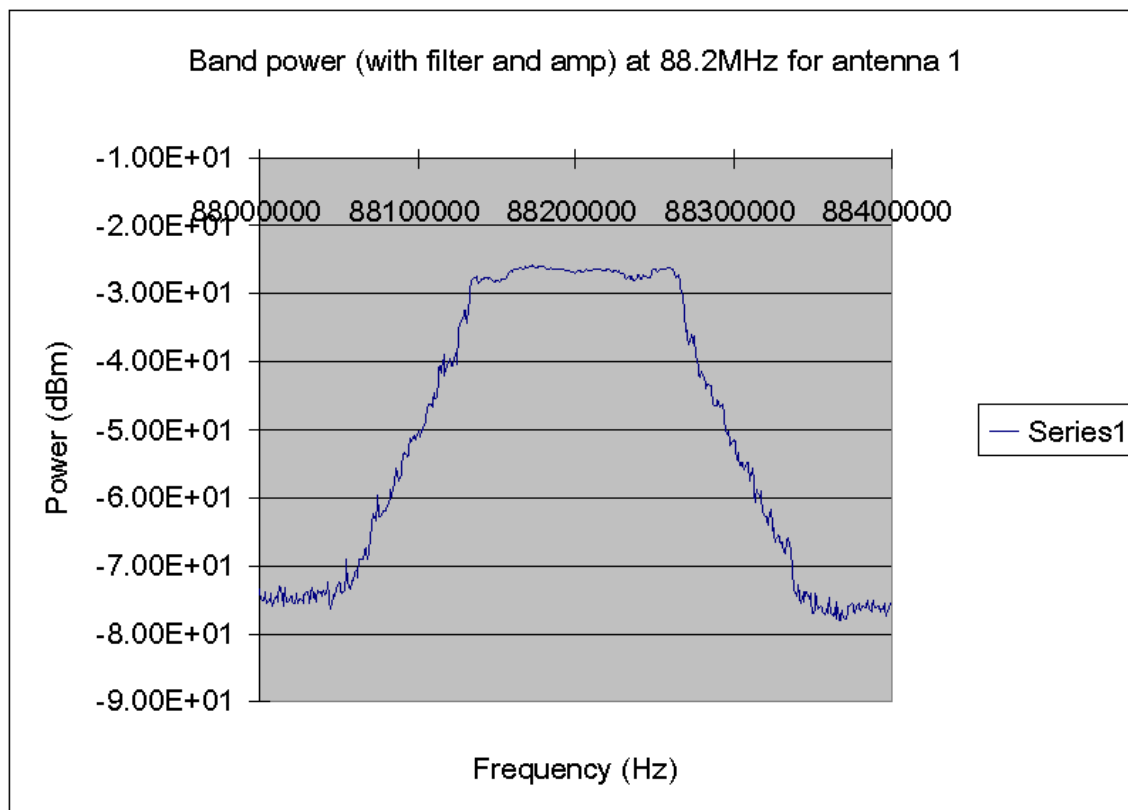


Figure 5.7: Band Power at 88.2MHz with Amplifier

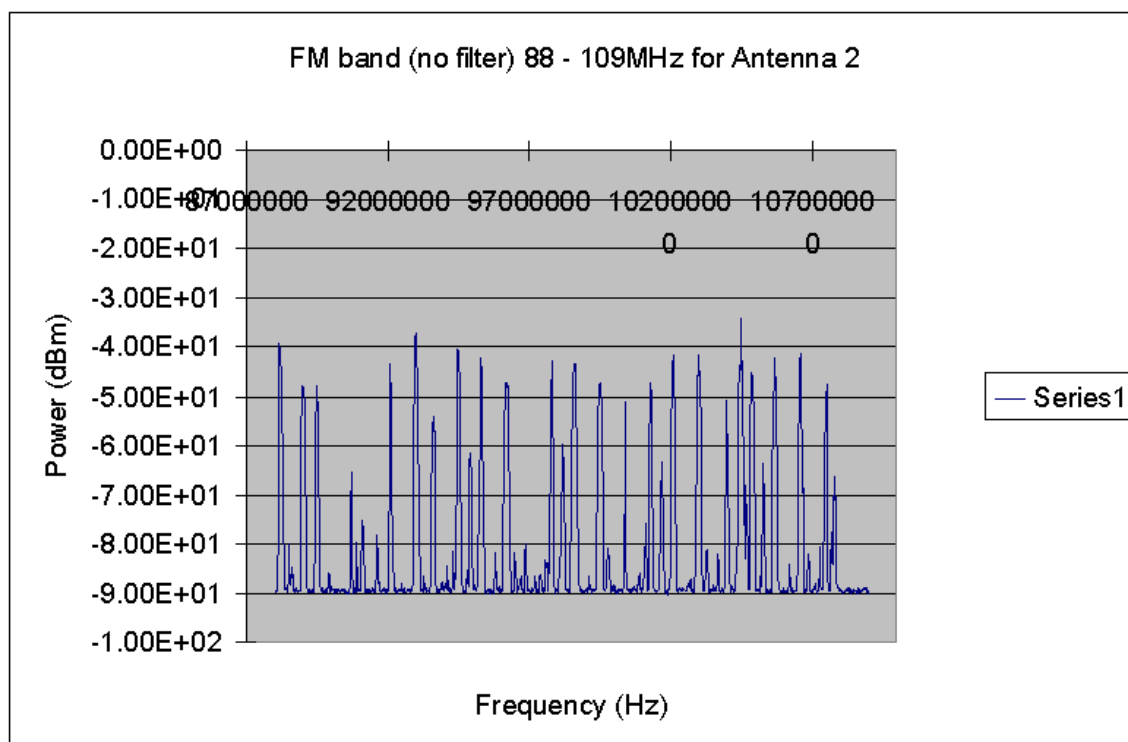


Figure 5.8: FM band

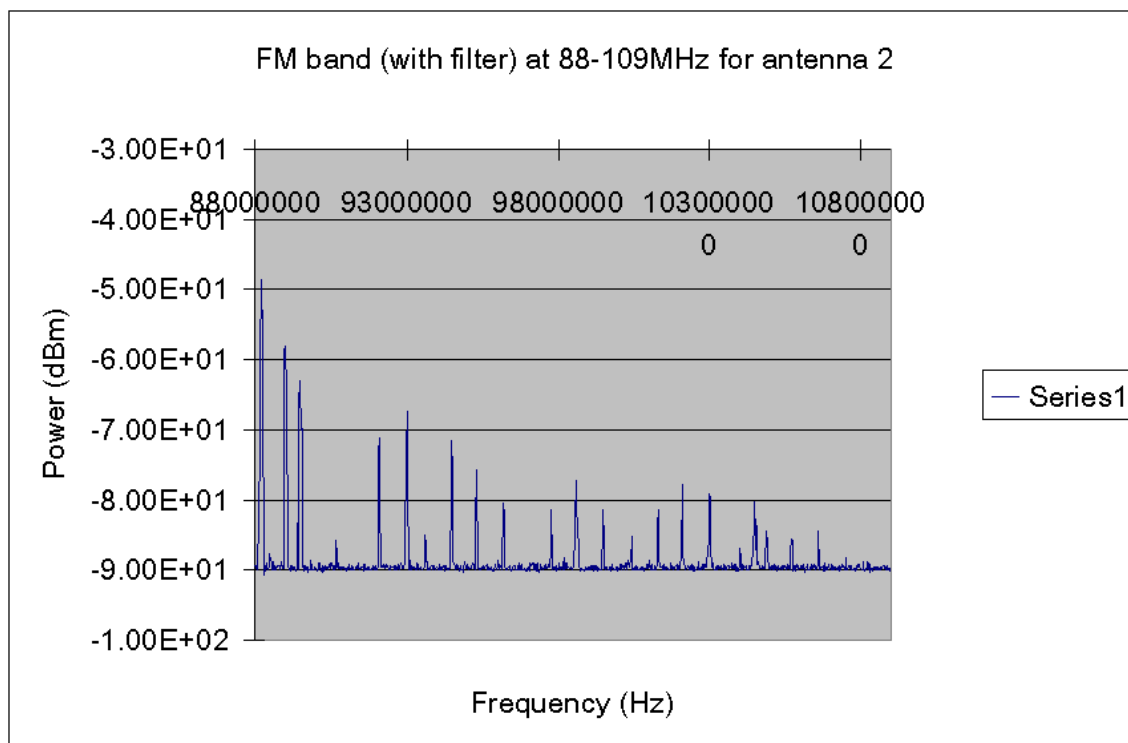


Figure 5.9: FM band with filter

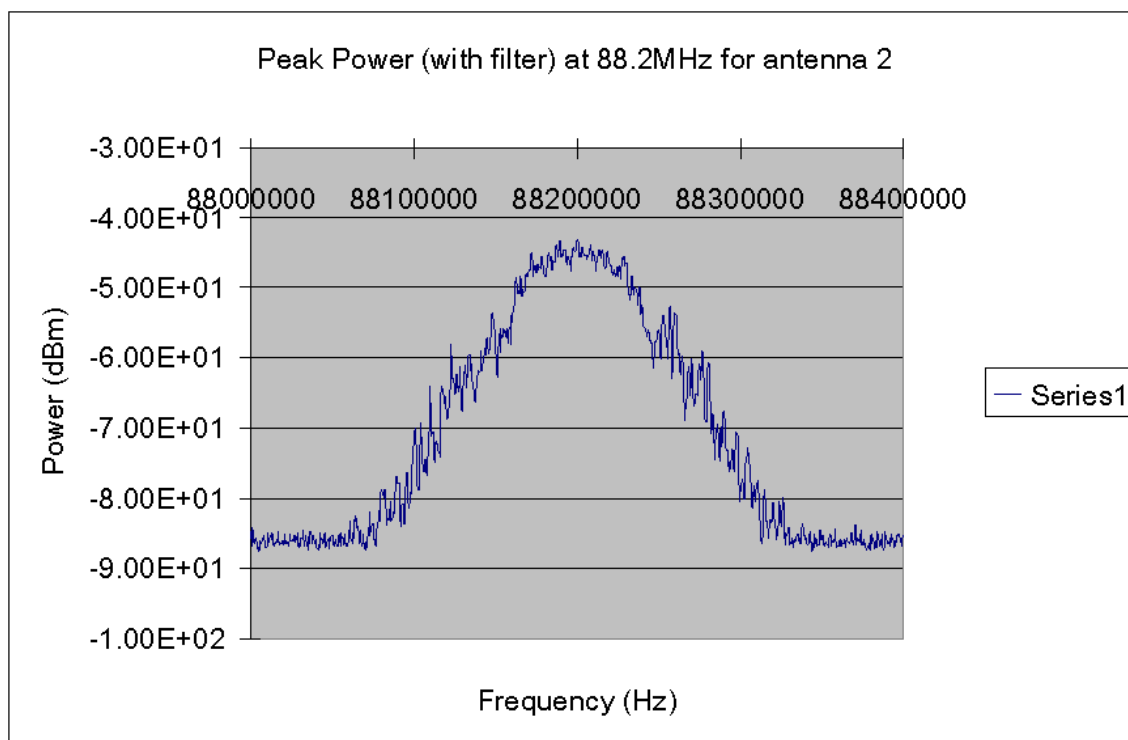


Figure 5.10: Peak power at 88.2MHz

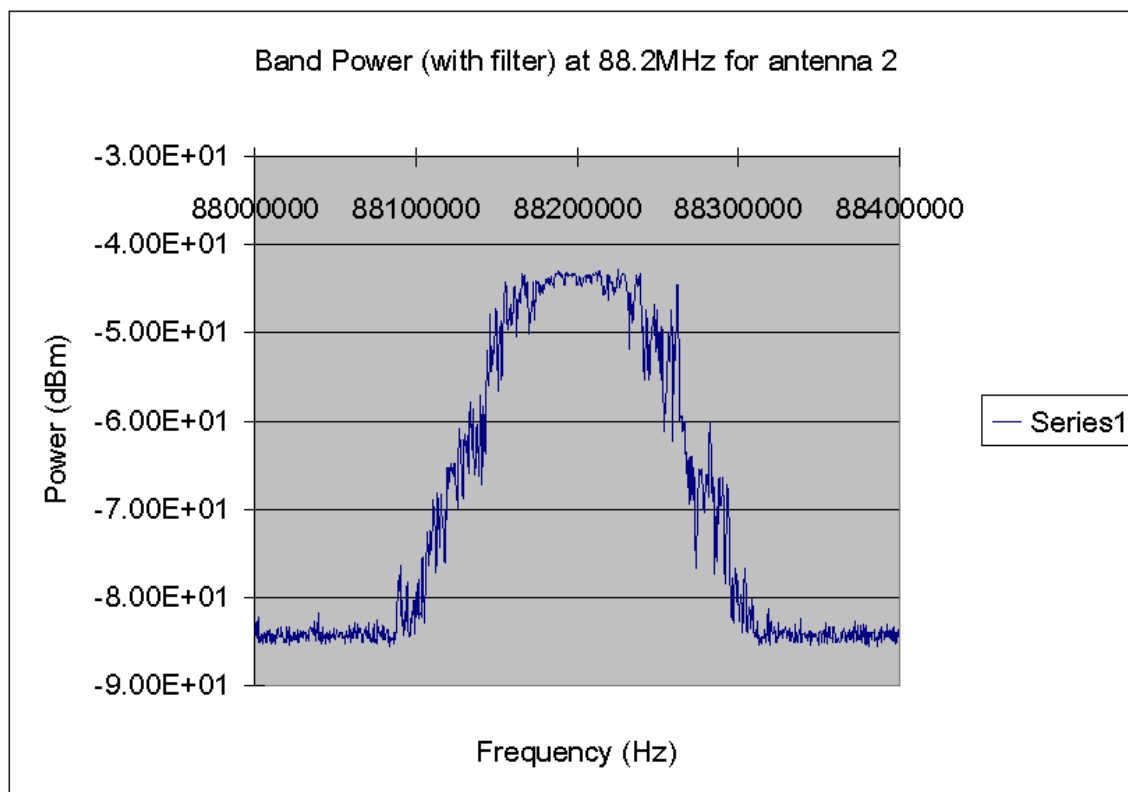


Figure 5.11: Band Power at 88.2MHz

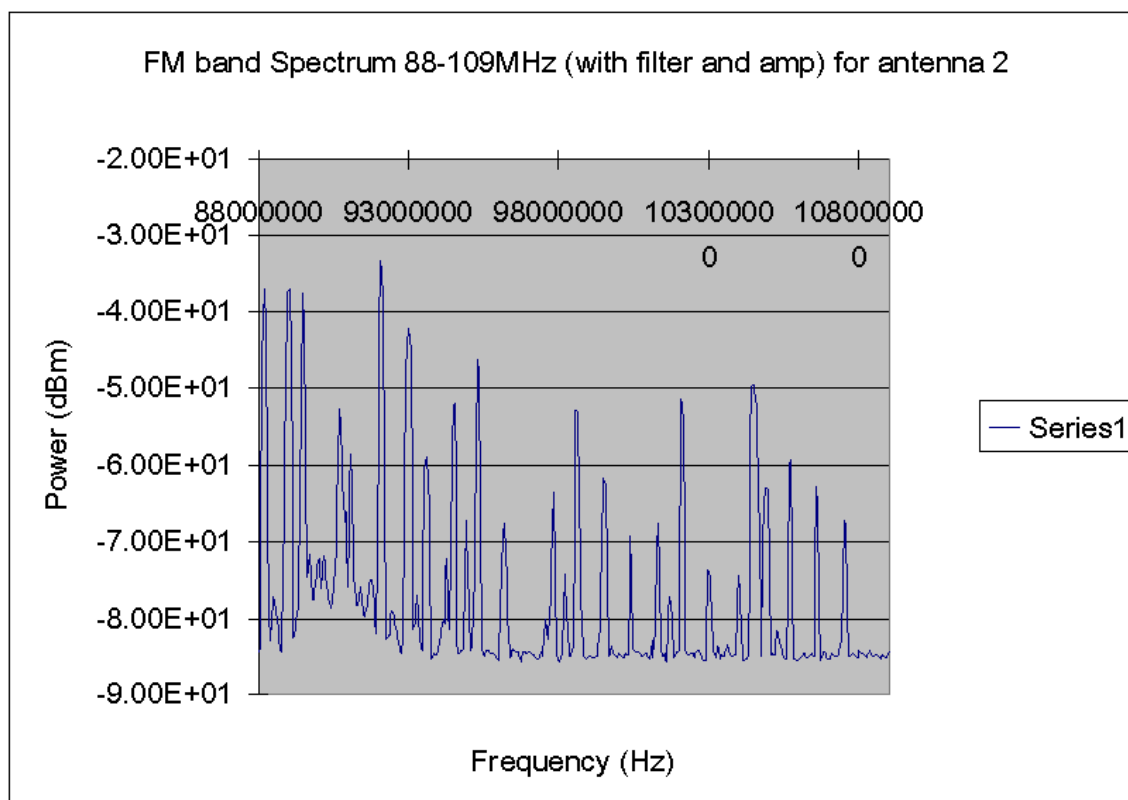


Figure 5.12: FM band

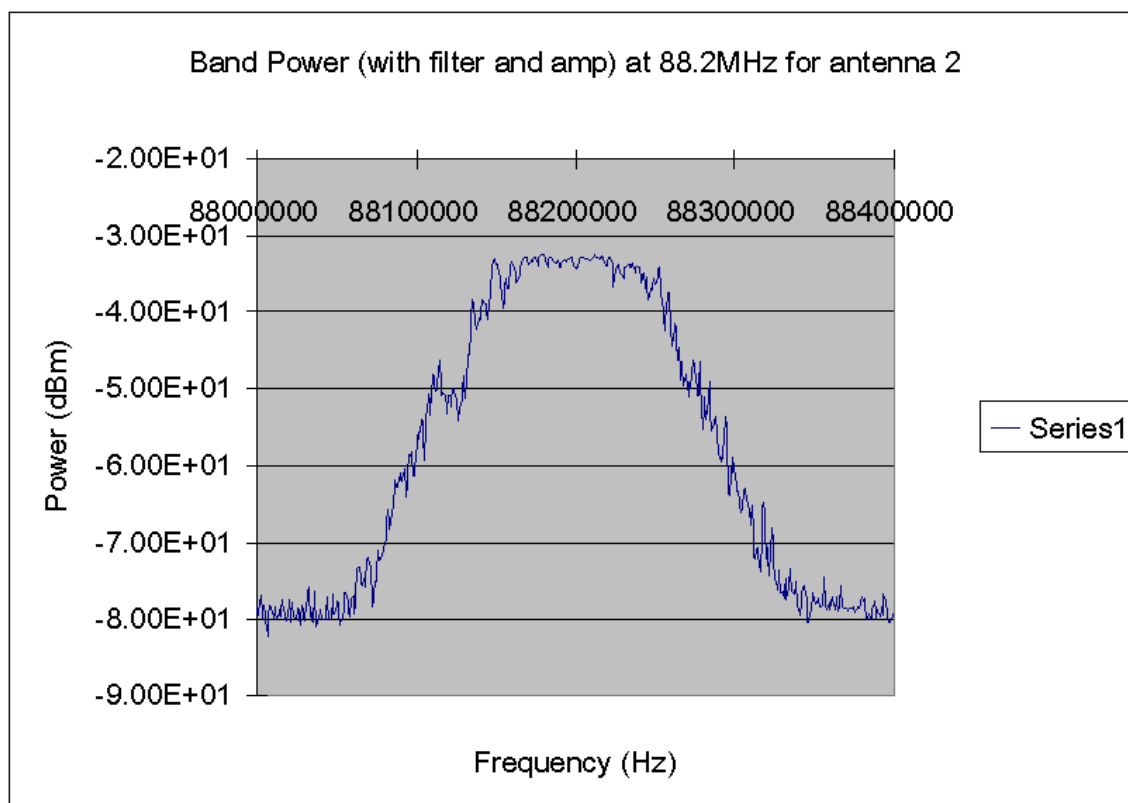


Figure 5.13: Band Power at 88.2MHz

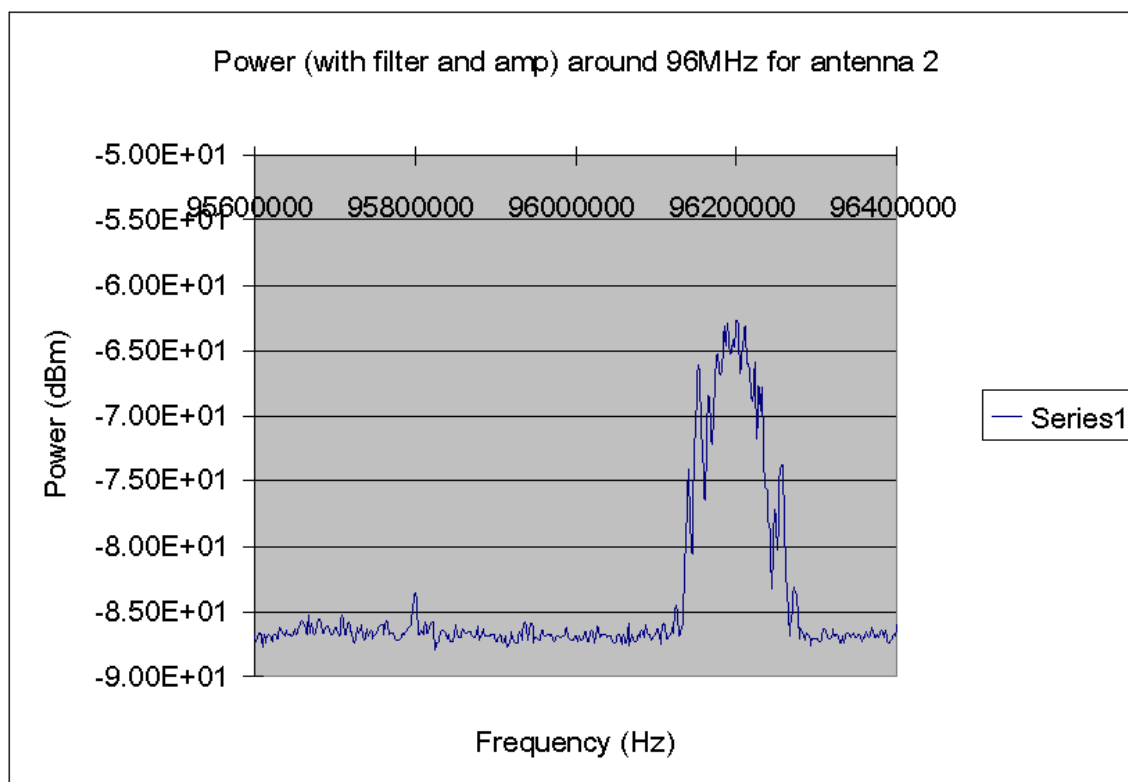


Figure 5.14: Power around 96MHz

- Band Power at 88.2MHz  $\rightarrow$ -36.84dBm
- Peak Power at 88.2MHz  $\rightarrow$ -50.52dBm

Antenna 1 (with filter and amplifier):

- Band Power at 88.2MHz  $\rightarrow$ -16.0dBm
- Band Power at 96MHz  $\rightarrow$ -52.0dBm

Antenna 2 (with filter):

- Band Power at 88.2MHz  $\rightarrow$ -30.40dBm
- Peak Power at 88.2MHz  $\rightarrow$ -43.22dBm

Antenna 2 (with filter and amplifier):

- Band Power at 88.2MHz  $\rightarrow$ -18.7dBm
- Band Power at 96MHz  $\rightarrow$ -52.04dBm

## 5.4 Final Experiment

### 5.4.1 Software

The GNU Radio built in software called GNU oscilloscope is used to check if any signals have been received in each channel. Channel 1 had responses and Channel 2 doesn't. This might be that the software was only written for one channel instead of two channels or the USRP is faulty. Figure 5.15 and 5.16 shows the response on the oscilloscope, the two waves shows the real and complex graphs.

The GNU Radio software for the basic RX boards has been written already, only some of the codes need to be modified. For the FM signal, 64 decimation rate is a better choice. The frequency must be adjusted to 88.2MHz and the number of samples adjusted to 9600000. In the USRP the frequency down converters to 24.2MHz from 88.2MHz. The DDC is set to -24.1MHz so there is a 100KHz shift if plotting in the frequency domain. The spacing between two antennas  $d = 1.2m$  and  $\lambda = 3.4m$

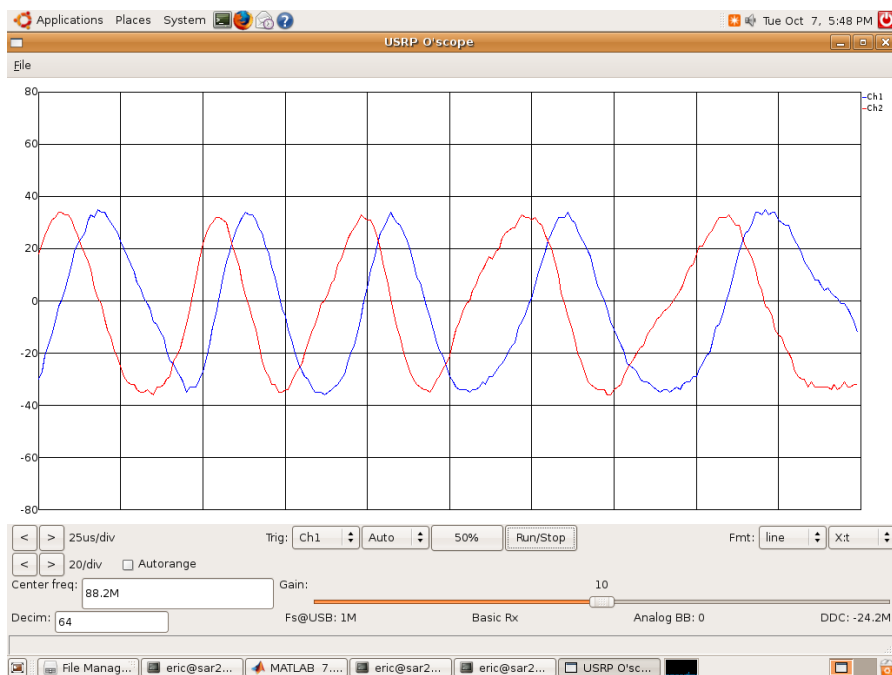


Figure 5.15: Real and Imaginary from scope

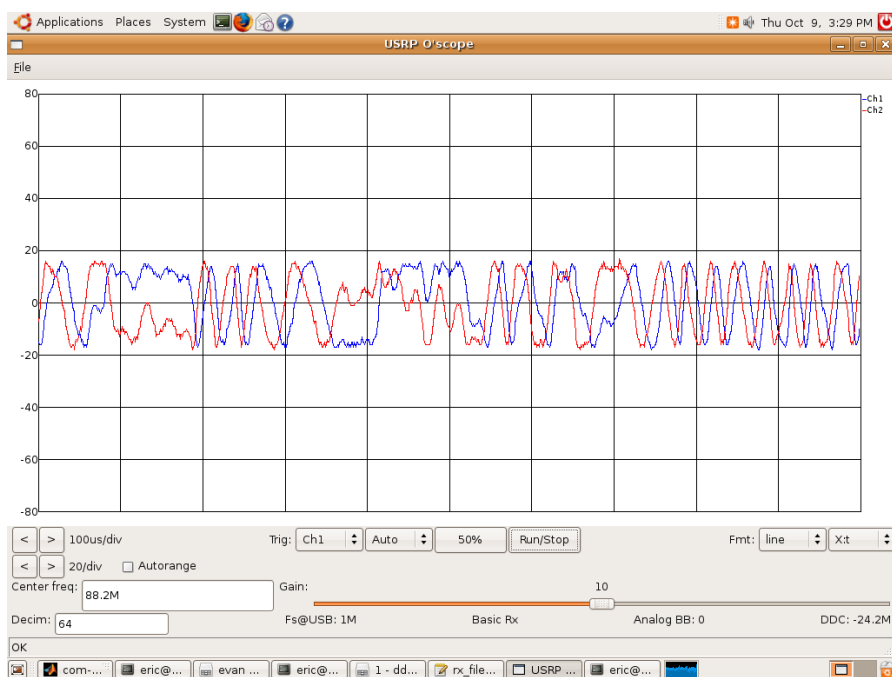


Figure 5.16: Real and imaginary (different time divisions)

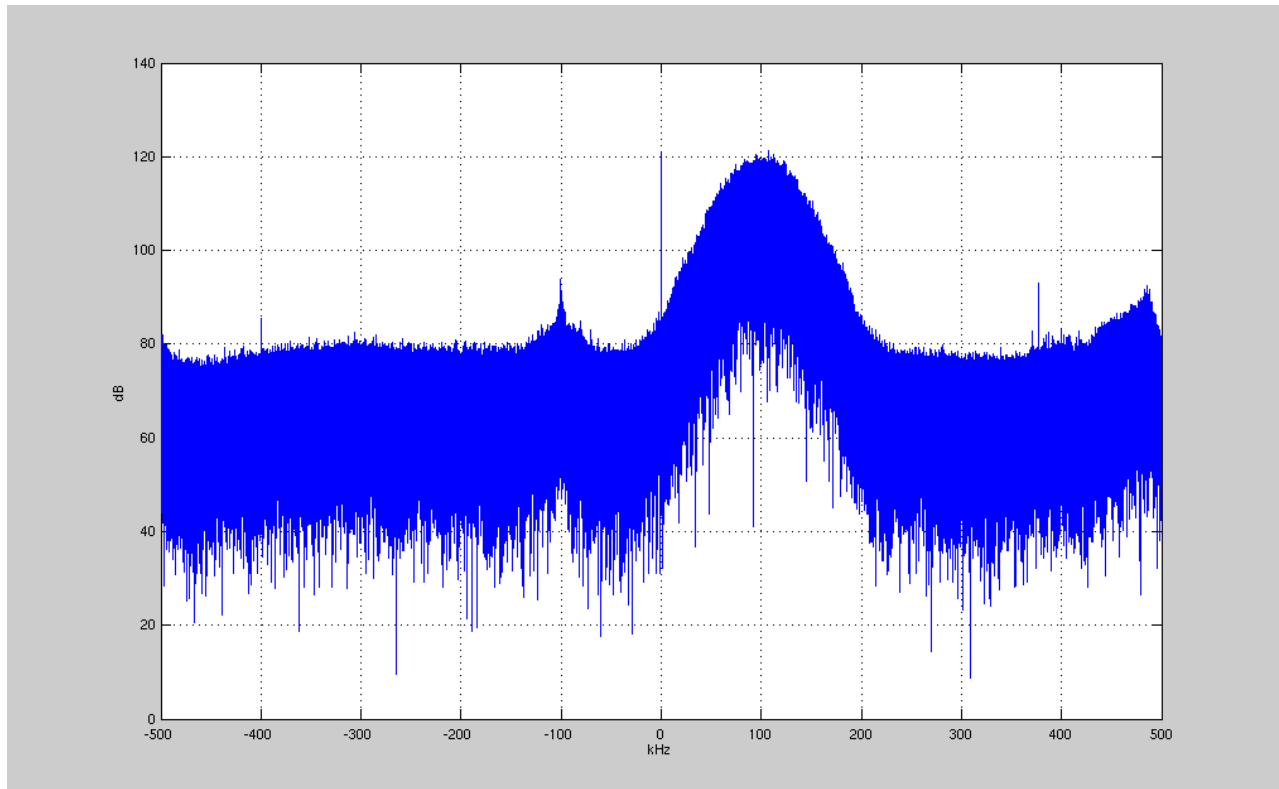


Figure 5.17: FFT of the signal received by the USRP (receiver)

## 5.4.2 Results

After digitising the signals from USRP. The data received can be process through MATLAB using the 'read\_complex\_binary.m' file. The 'read\_complex\_binary.m' function converts the digitised signal to complex binaries. After processing the data, the interferometer phase difference techniques can be applied to find the angle of arrival. Figure 5.17 shows the FFT of the signal when the DDC is set to -24.1MHz, so it will be centred at 100kHz because our DXC is at -24.2MHz.

Taking the mean phase of the both signals and subtracting the one to the other, the results were

$$\Delta\psi = -5.1444 = -5.144 + 2\pi = 1.1388.$$

Using equation 2.2 , the angle of arrival will be  $\phi = \arcsin(1.1388 \times 3.4/2\pi(1.2)) = 30.9^\circ$

So the angle of interest will be  $90^\circ - 30.9^\circ = 59.1^\circ$

The results shown is not the result that was expected. The angle of arrival should be around  $38^\circ$ . The problem might be with the antennas. Yagi antennas might cause interference with one another to introduce another phase delay. This might be the problem the readings are very poor. All other components are checked to ensure that no other phase delays can happen so the problem might just be with the antenna. Due to the time limitations, no further experiment could be done. The other problem might be the filter that causes time delay because of the  $\delta$  function. The filter is not perfectly identical, so it might cause different time delays that will also cause phase differences. This might not be a big problem because the wavelength is 3m so even if theres a phase difference, it will not



have a big influence on the reading.

# Chapter 6

## Conclusions

- Modern direction finding system is a very useful tool used to find the angle of arrival of a signal (electromagnetic wave).
- Triangulation technique perform well in terms of accuracy, the variance is around  $0.25^\circ$ . Triangulation technique does not just find the angle of arrival but also the location of the transmitter or a moving target.
- Interferometer technique perform very well in terms of accuracy, the variance is around  $0.05^\circ$ . Interferometer technique can only find the angle of arrival and not the position of the transmitter or moving targets.
- In practise, there will be many error sources that will occur during the transmission process. The general errors that occurred are propagation-induced errors where there are disturbances such as the surface of the earth from the transmitter to receiver not being flat and instrumentation errors where the received signal is too weak even after amplifying the signal.
- In practise, the interferometer antenna array must be perfectly aligned to each other to get a more accurate reading of the angle of arrival, which is not possible because the antenna cannot be perfectly aligned in practise. The antennas might be misaligned by wind or gravity. The other causes of error might be that the two antennas are not perfectly identical and that the cables are not perfectly the same length. Both of these problems can contribute to the bad results.
- Both triangulation and interferometer techniques are useful to find the angle of arrival of a received signal. Interferometer is a cheaper and easier way to find the angle of arrival because it only needs one antenna site. Triangulation technique is much more complicated because several receivers are needed far away from one another to get a better accuracy, but this technique can locate the position of the transmitter.

# Chapter 7

## Future Work

- More experiments need to be done in order to make sure that the interferometer technique will give an accurate reading after experiencing the error sources that might occur during the experiment.
- More direction finding technique should be researched and implemented.
- Better wires and coils should be used to construct the bandpass filter to prevent high losses. High filter losses will influence the receiver from capturing the data because the signals will be too weak.
- High gain amplifier should be used instead of a 20dB gain amplifier because the signal was still too weak after amplification.
- Testing both techniques used in this project on the moving target which was not covered in this project.
- Triangulation technique experiments should be done to see how accurate the technique can get.
- Filters should be built as accurate as possible for any experimentation
- Change the Yagi antennas to dipole antennas for the interferometer experimentation to check if it gives a better result.

# Appendix A

## Software Source Code

All software code (Matlab, FERS and Python) is in the CD provided with the project report.

'eqn.m' file is used to process the data for triangulation to get the angle of arrival and locate the position of transmitter.

'ang.m' file is used to check the phase difference of the interferometer technique to find the angle of arrival of the signal.

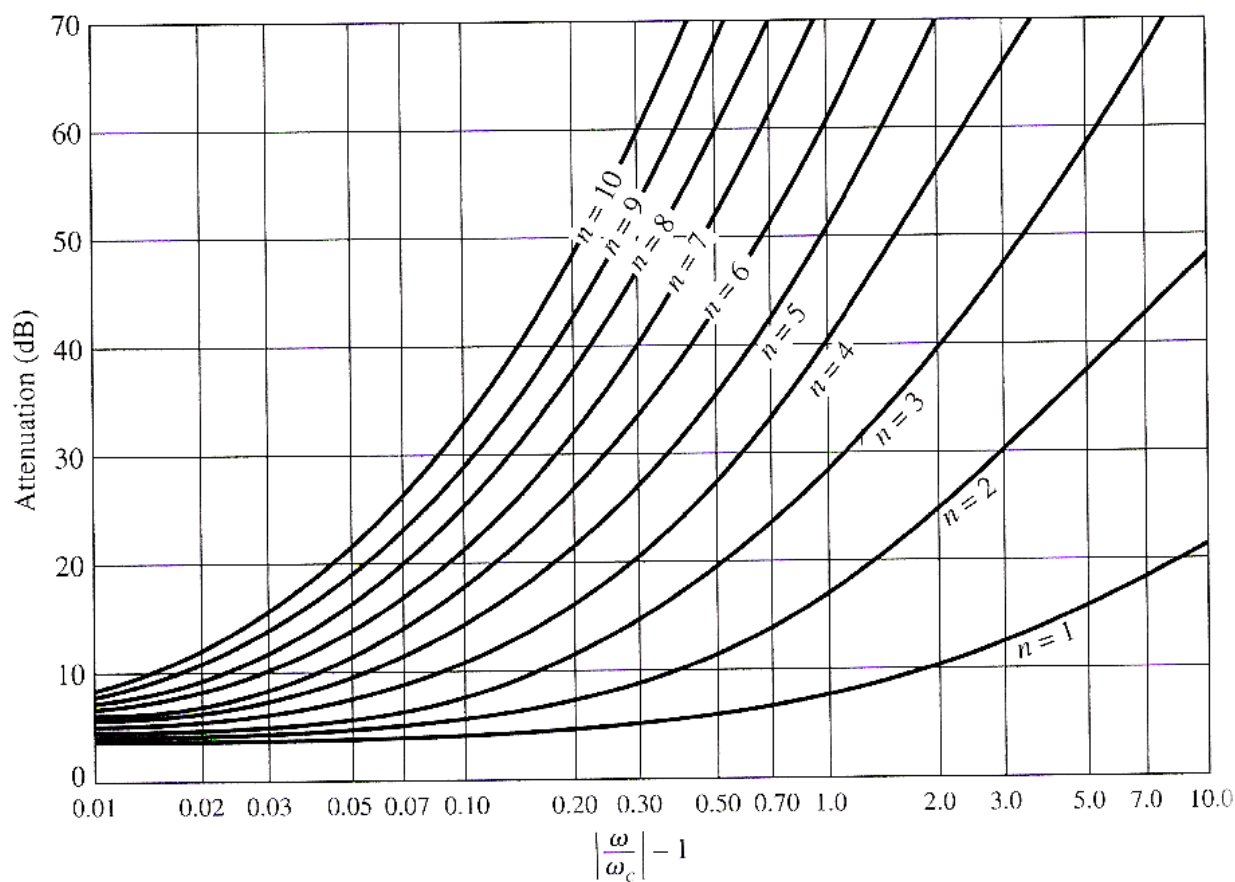


Figure A.1: Attenuation versus normalised frequency for 3.0dB ripple level [9]

3.0 dB Ripple

$N$	$g_1$	$g_2$	$g_3$	$g_4$	$g_5$	$g_6$	$g_7$	$g_8$	$g_9$	$g_{10}$	$g_{11}$
1	1.9953	1.0000									
2	3.1013	0.5339	5.8095								
3	3.3487	0.7117	3.3487	1.0000							
4	3.4389	0.7483	4.3471	0.5920	5.8095						
5	3.4817	0.7618	4.5381	0.7618	3.4817	1.0000					
6	3.5045	0.7685	4.6061	0.7929	4.4641	0.6033	5.8095				
7	3.5182	0.7723	4.6386	0.8039	4.6386	0.7723	3.5182	1.0000			
8	3.5277	0.7745	4.6575	0.8089	4.6990	0.8018	4.4990	0.6073	5.8095		
9	3.5340	0.7760	4.6692	0.8118	4.7272	0.8118	4.6692	0.7760	3.5340	1.0000	
10	3.5384	0.7771	4.6768	0.8136	4.7425	0.8164	4.7260	0.8051	4.5142	0.6091	5.8095

Source: Reprinted from G. L. Matthaei, L. Young, and E. M. T. Jones, *Microwave Filters, Impedance-Matching Networks, and Coupling Structures* (Dedham, MA: Artech House, 1980), with permission.

Figure A.2: Element values for 3.0dB Equal Ripple low-pass Filter Prototypes [9]

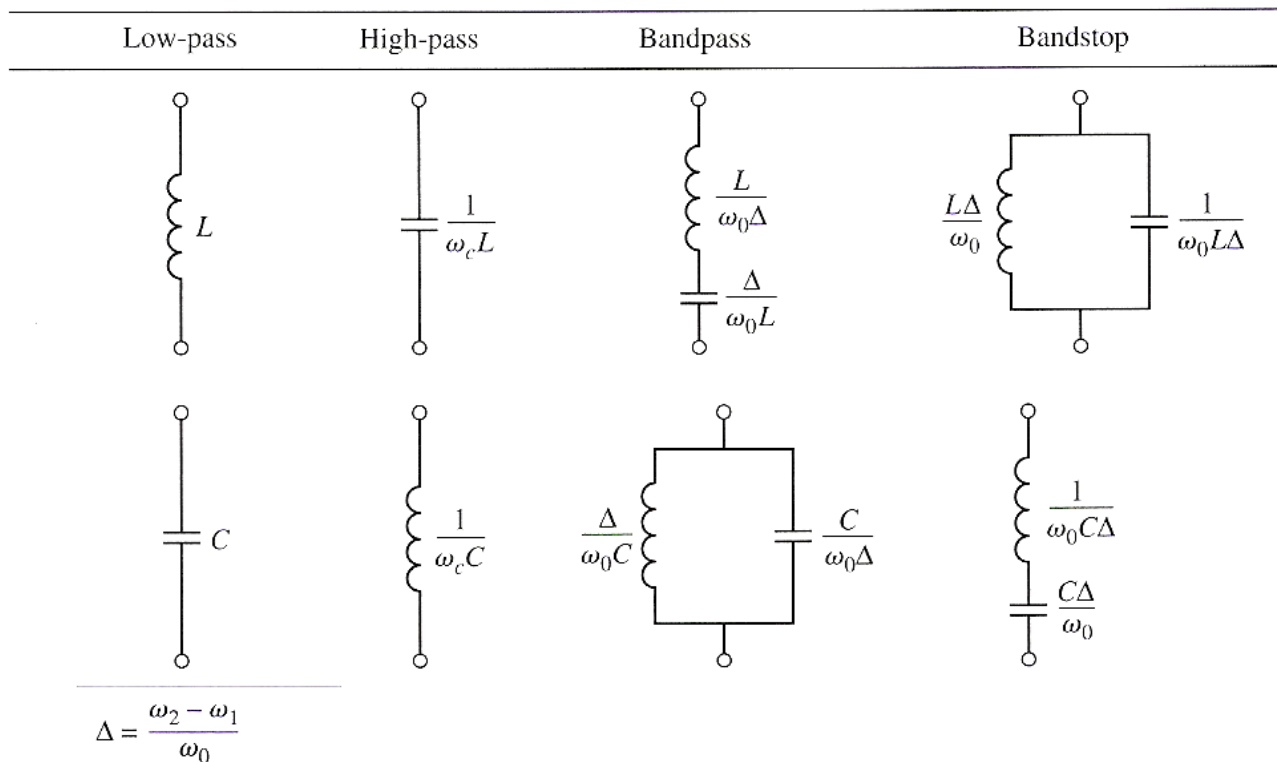


Figure A.3: Prototype Filter Transformation [9]



Figure A.4: Bandpass filter construction

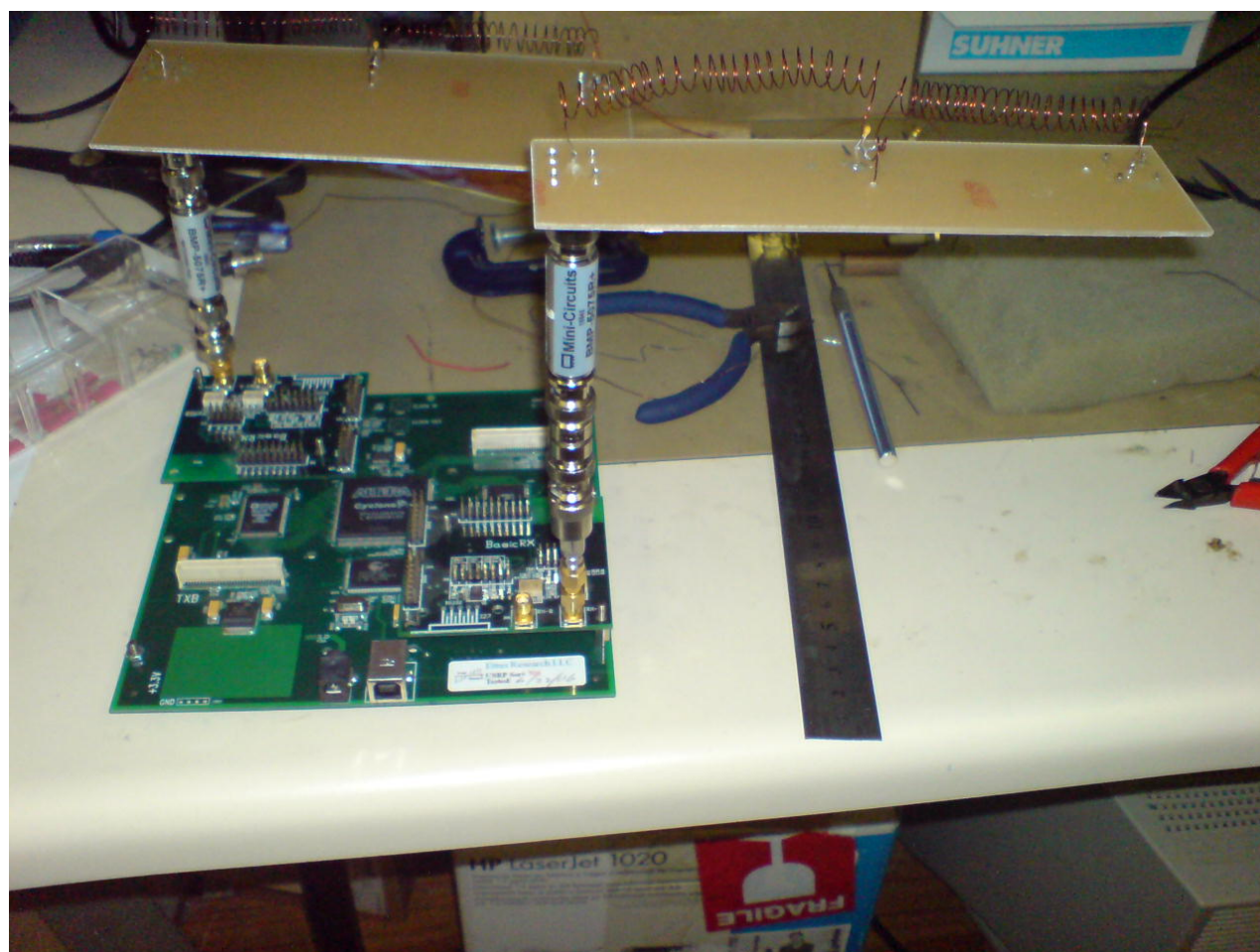


Figure A.5: Receiver construction

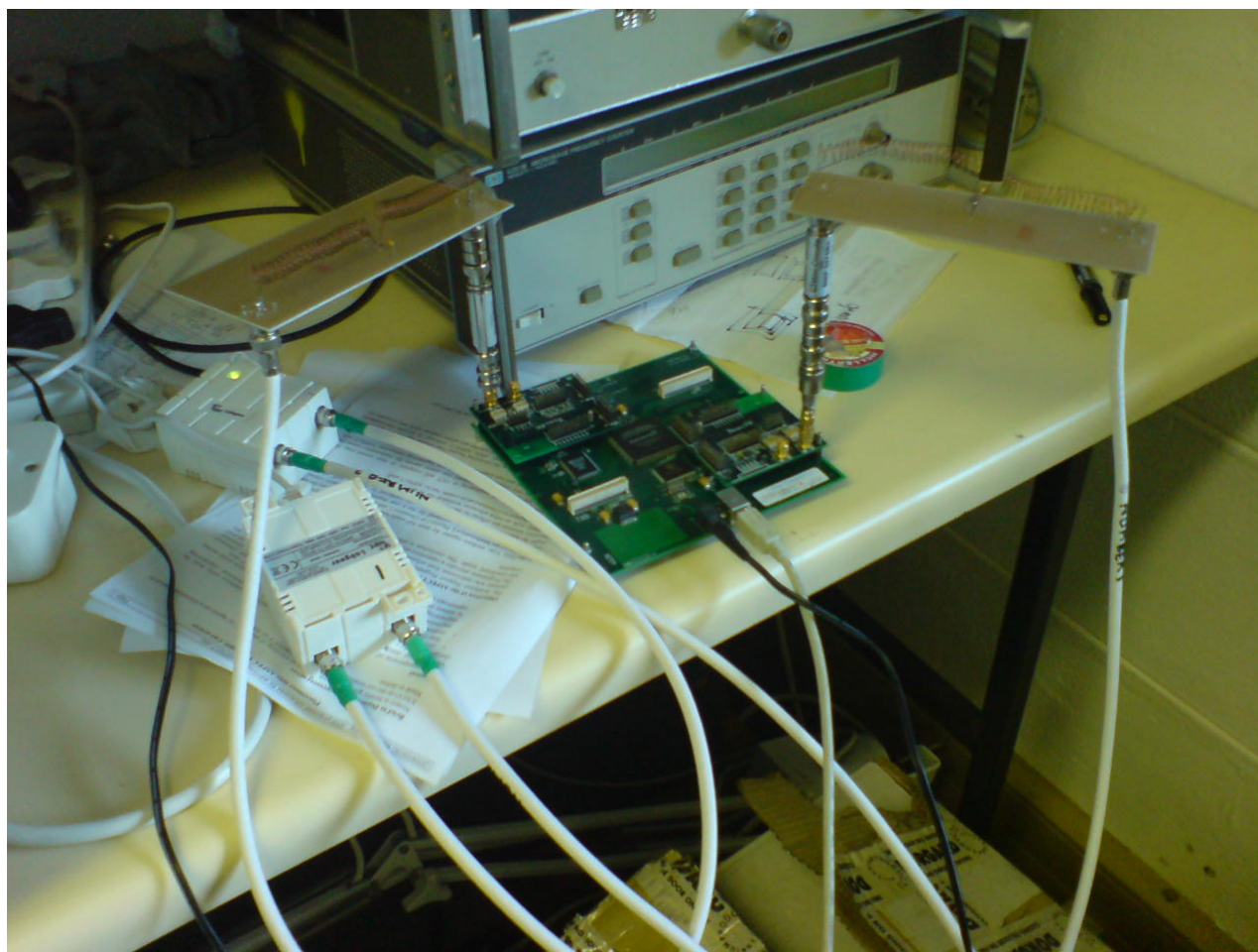


Figure A.6: Receiver construction

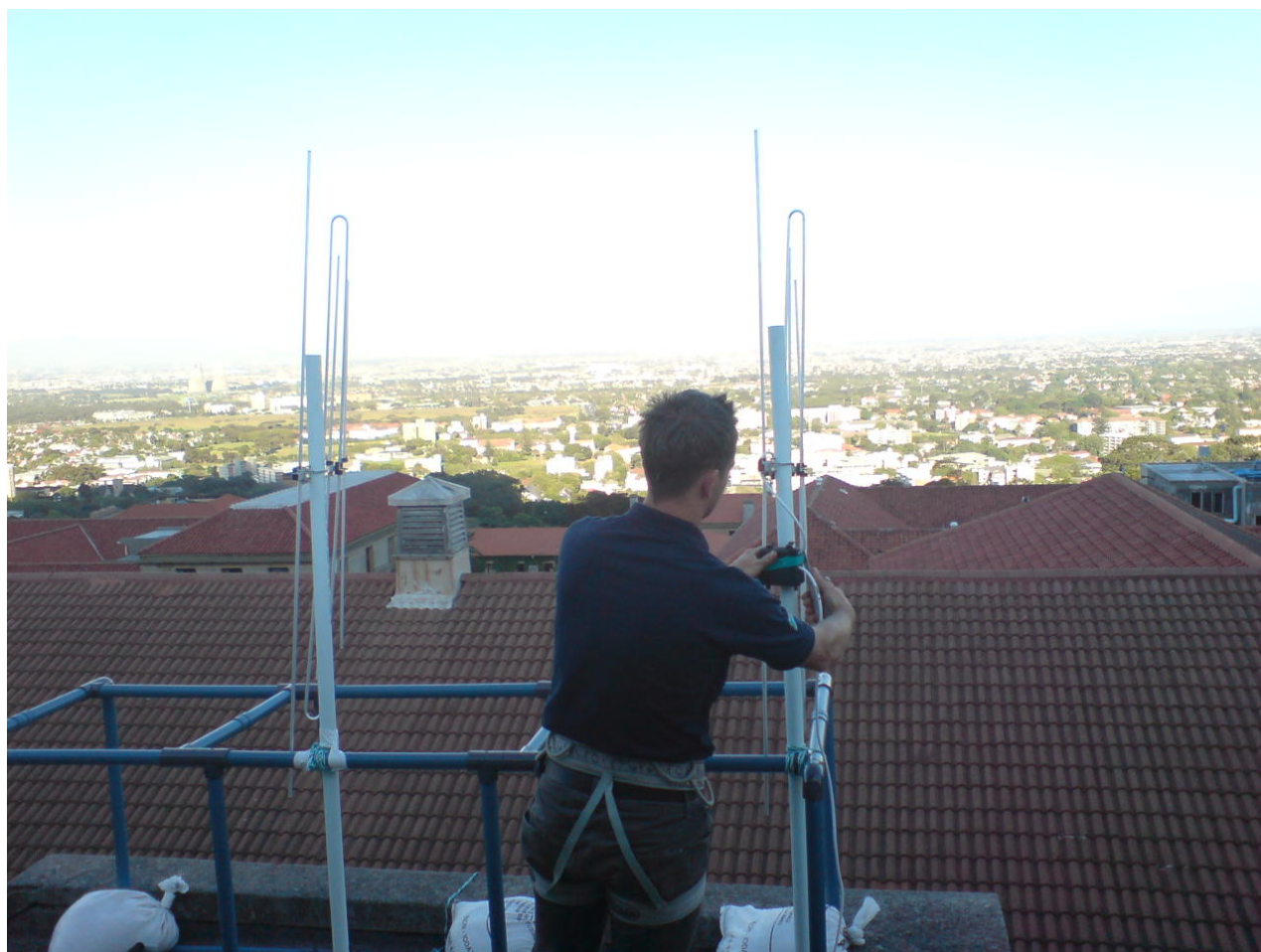


Figure A.7: 2 Array Yagi Antenna

# Bibliography

- [1] Signal sorting methods and direction finding. October 2008.
- [2] R. Bucher and D. Misra. A synthesizable vhdl model of the exact solution for three-dimensional hyperbolic positioning system. Master's thesis, Department of Electrical and computer engineering, New Jersey Institute of Technology, 2001.
- [3] D. Durrett. Dsss detection and direction finding methods for a dsp-based small aperture df system. Master's thesis, University of Cape Town, 2005.
- [4] N. Y. Guler. Indoor source localization via direction finding technique. Master's thesis, Sabanci University, 2004.
- [5] H. H. Jenkins. *Small-Aperture Radio Direction-Finding*. Artech House, Inc., 1991.
- [6] J. M. Kristensen. Gnu radio an introduction. 2007.
- [7] L. R. Paradowski. Microwave emitter position location: present and future. 4:97–116, 1998.
- [8] P. Balister and J. Reed. Usrc hardware and software description. Technical report, Virginia Polytechnic Institute & State University, 2006.
- [9] D. M. Pozar. *Microwave and RF Design of Wireless Systems*. John Wiley & Sons, INC., 2001.
- [10] E. Stansfield. Accuracy of an interferometer in noise. 143:217–226, august 1996.